Identification and characterisation of genes for hair disorders

Doctoral thesis

to obtain a doctorate (PhD)

from the Faculty of Medicine

of the University of Bonn

Nicole Cesarato

from Dolo, Italy

2024

Written with authorization of

the Faculty of Medicine of the University of Bonn

First reviewer: Prof. Dr. med. Regina C. Betz

Second reviewer: Prof. Dr. med. Jorge Frank

Day of oral examination: 27.05.2024

From the Institute of Human Genetics

Director: Prof. Dr. med. Markus M. Nöthen

Table of Contents

List of abbreviations

CNV	Copy number variation
DNA	Deoxyribonucleic acid
ED	Ectodermal dysplasia
GWAS	Genome-wide association study
HF	Hair follicle
HS	Hypotrichosis simplex
MPHL	Male pattern hair loss
PCR	Polymerase chain reaction
RNA	Ribonucleic acid
SAH	Short anagen hair
SNV	Single nucleotide variation
UHS	Uncombable hair syndrome
WES	Whole exome sequencing

1. Abstract

Hair disorders comprise conditions in which affected individuals display one or more of the following features: an absence or a reduced amount (e.g. hypotrichosis) of hair; an excessive amount of hair (e.g. hypertrichosis); abnormal hair structure (e.g. uncombable hair syndrome, UHS); or abnormal hair growth (e.g. short anagen hair, SAH). Hair disorders develop as a consequence of genetic and/or environmental factors. The nature of the genetic influences can be either: i) direct causality as in the case of monogenic diseases, as in UHS or hypotrichosis; or ii) genetic susceptibility, as in male pattern hair loss (MPHL) also termed androgenetic alopecia. While causal or susceptibility genes have already been identified for some hair phenotypes, others still await molecular genetic elucidation.

Therefore, the primary aim of the research described in the present thesis was to identify novel variants and/or genes associated with hair disorders.

Within the context of a total of three separate studies, we performed Sanger and/or whole exome sequencing in DNA from patients affected by clinically diverse hair disorders, namely, hypotrichosis, UHS, and SAH. We identified novel pathogenic variants in genes that had already been associated with hypotrichosis and UHS and, for the first time, elucidated the genetic background of SAH by identifying a novel gene associated with its development. In detail, we identified novel pathogenic variants in *LSS* in four individuals affected by hypotrichosis with or without intellectual disability. We identified novel pathogenic variants in *PADI3*, *TGM3*, and *TCHH*, three genes associated to UHS, and delineated the mutational spectrum of UHS in a large cohort of 107 individuals. We performed molecular genetic analyses in a cohort of 48 individuals with SAH, and we discovered rare or low-frequency *WNT10A* variants in mono- or bi-allelic state in 20 of them. Using population-based genetic data we demonstrated the significant enrichment of *WNT10A* variants in individuals with SAH and discovered that two of the SAH-associated *WNT10A* variants are also associated with the risk of developing MPHL and partially explain the known association between *WNT10A* and MPHL.

With these results, we have expanded knowledge on genetic hair disorders. In particular, we have: i) broadened the genetic spectrum of *LSS*-associated hypotrichosis; ii) delineated the mutational spectrum of UHS; and iii) unravelled that SAH has a genetic component by showing its association with *WNT10A* variants.

2. Introduction and aims with references

2.1 Hair follicle anatomy, function, morphogenesis, and cycle

The hair follicle (HF) is a complex mini organ of the skin that produces the hair shaft. In mammals, hair is involved in a wide range of functions, such as thermal insulation, sensation, and physical protection. In human societies, hair is of major psychosocial importance (Paus und Cotsarelis, 1999; Schneider et al., 2009).

The HF is formed by several cell types (e.g. keratinocytes, melanocytes, dermal papilla cells, stem cells), which are organised into specific structures. These comprise the hair shaft itself, which is surrounded by the inner and outer root sheath; the hair bulge, which contains the stem cells; and the dermal papilla, which contains mesenchymal cells of importance in terms of cell proliferation and differentiation. Together with a sebaceous gland, an apocrine gland, and an arrector pili muscle, the HF constitutes the pilosebaceous unit (Figure 1) (Schneider et al., 2009).

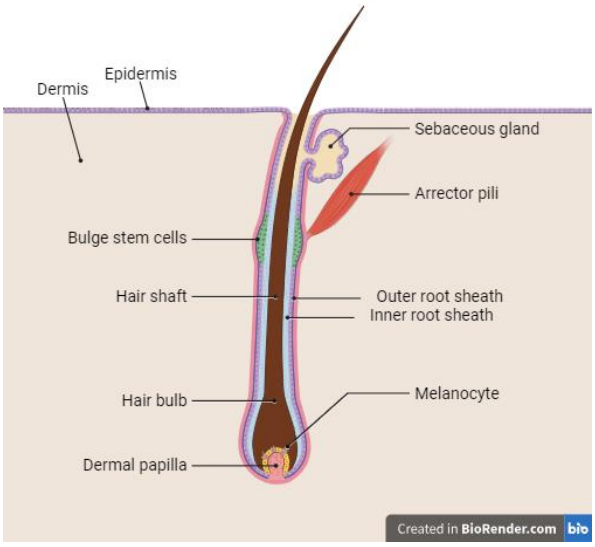

Fig. 1. Pilosebaceous unit schema. (Created with BioRender.com)

All of these structures arise during HF morphogenesis in the embryo, from the cross-talk between the ectoderm (epidermis) and the mesoderm (dermis). Studies in mice have shown that while the dermis is responsible for the induction of hair morphogenesis, a concert of signals between epidermis and dermis is required for the orderly proliferation of both cell populations. Essential signalling pathways for hair morphogenesis include Wnt, BMP, Fgf, EDA-EDAR, TGFβ, and Shh (Lin et al., 2022; Millar, 2002; Paus et al., 1999; Rishikaysh et al., 2014; Saxena et al., 2019).

After birth, the HFs produce hair strands via undergoing cycles of growth (anagen), apoptosis-mediated regression (catagen), and relative quiescence (telogen). In each cycle, a new hair shaft is formed, while the existing one is shed in a process called exogen. This cycle is finely regulated, whereby the generation of a new hair shaft depends on the activation of hair-specific stem cells contained in the bulge region of the HF. Fine-tuned activation of different signalling pathways, such as Wnt, Notch, BMP, and shh, allows both the generation of all HF structures and regression in the catagen phase (Schneider et al., 2009). Under normal conditions, 90% of human HFs are in the anagen phase, which lasts from 2 to 5 years. Both the ability of the HF to form the hair shaft, and the length of the HF cycle, can change depending on pathologies, use of drugs, and physiological conditions.

2.2 Genetic hair disorders

Genetic hair disorders comprise a number of conditions in which affected individuals display the absence of hair (alopecia/hypotrichosis), an excessive amount of hair (hirsutism/hypertrichosis), an abnormal hair shaft (e.g. uncombable hair syndrome), and/or an abnormal HF cycle (e.g. short anagen hair). In general, hair disorders can have a profound adverse psychological impact on affected individuals (Randolph et al., 2022; Toussi et al., 2021).

Hair disorders have highly diverse genetic backgrounds. Some are monogenic in nature, for example hypotrichosis. Here, the disorder is caused by mono- or biallelic pathogenic variants in a single gene that is essential for HF morphogenesis, HF function, and/or the hair cycle (Duverger und Morasso, 2014). Other hair disorders have a polygenic (e.g. male pattern hair loss), or multifactorial (e.g. alopecia areata) background (Betz et al., 2015; Yap et al., 2018). Here, multiple genetic and environmental factors contribute to disease aetiopathogenesis. In some hair disorders, the genetic background has not yet been elucidated.

2.2.1 Hypotrichosis

Hypotrichosis is characterised by diffuse and progressive loss of scalp and/or body hair, eyebrows, and eyelashes, and encompasses a group of rare monogenic hair disorders. When hypotrichosis occurs as an isolated phenotype, with no hair shaft abnormality, it is termed hypotrichosis simplex (HS). Syndromic forms of hypotrichosis have also been

described, in which tissues other than hair are also affected. In both cases, autosomal dominant and recessive forms have been reported, depending on the mutated gene.
Consistent with the physiological complexity of the HF, causal pathogenic variants in genes involved in various signalling pathways have been reported for hypotrichosis (simplex and syndromic). The most frequently affected cellular components and signalling pathways are: transcription regulation (e.g. *SOX18*, *LEF1*, *HOXC13*), keratin network (e.g. *KRT81*, *KRT83*, *KRT86*), cell-cell adhesion (e.g. *DSG4*, *DSC3, CDH3*), lipid and sterol synthesis and homeostasis (e.g. *LIPH*, *LPAR6*, *SREBF1*, *LSS*), splicing (e.g. *SNRPE*), the EDA/EDAR pathway (e.g. *EDA*, *EDAR*, *EDARADD*), and the Wnt pathway (e.g. *LEF1*, *WNT10A, APCDD1*) (Duverger und Morasso, 2014).
LSS is an example of a gene that is associated with both HS and syndromic forms of hypotrichosis/alopecia. *LSS* is widely expressed in human tissues, comprising hair and skin, and codes for lanosterol synthase. The latter is an enzyme that catalyses the conversion of (S)-2,3 oxidosqualene to lanosterol, which is the first step in cholesterol biosynthesis. Biallelic *LSS* pathogenic variants can cause five clinically distinct phenotypes: cataract, mutilating palmoplantar keratoderma, hypotrichosis, alopecia-intellectual disability syndrome, and palmoplantar keratoderma-congenital alopecia syndrome. In the latter three phenotypes, hair is always affected. Individuals with an *LSS*-related disorder can present with cataract, palmoplantar keratoderma, keratosis, hypogenitalism, agenesis of the corpus callosum, epilepsy, and/or intellectual disability. However, current understanding of the genotype-phenotype correlations of *LSS* variants remains limited (Besnard et al., 2019; Romano et al., 2018; Yang et al., 2022; Zhao et al., 2015; Zhou et al., 2023).

2.2.2 Uncombable hair syndrome

Uncombable hair syndrome (UHS) is a hair shaft anomaly that presents with dry, frizzy, wiry, and often light-coloured and shiny hair that stands out from the scalp and cannot be combed flat. UHS frequently improves with age. On microscopic evaluation, UHS hair shafts have typical longitudinal grooves and a heart-shaped cross-section. Genetically, UHS is a monogenic disorder that is associated with autosomal recessive pathogenic variants in *PADI3*, *TGM3*, and *TCHH*. These three genes encode for proteins that participate in the formation of the hair shaft. In particular, trichohyalin (TCHH) is a

structural protein of the hair shaft. Only after its deimination by PADI3 can TCHH be crosslinked to the keratin filaments by TGM3. This molecular process is necessary for the stabilisation and hardening of the hair shaft, and disruption of any of the players in this process leads to UHS (Ü Basmanav et al., 2016).

2.2.3 Short anagen hair syndrome

Short anagen hair (SAH) is a hair abnormality that is characterised by a short anagen phase of the HF, which manifests as the inability to grow long scalp hair. In individuals with SAH, hair length is restricted to around 3-10 cm due to an estimated anagen duration of 4-10 months. SAH mostly affects females aged 3-6 years, and may improve with age and resolve after puberty (Oberlin et al., 2018). SAH has a strong adverse psychological and emotional impact on affected children and their parents. Around half of all SAH-affected individuals and their parents report negative psychological symptoms (Randolph et al., 2022). The exact prevalence of SAH is unknown. However, SAH is considered a rare condition, and prior to our investigation, its genetic background had not yet been clarified.

2.2.4 Male pattern hair loss

Male pattern hair loss (MPHL), also termed androgenetic alopecia, is the most common of all human hair disorders, and affects up to 80% of Caucasian men. MPHL is androgen-dependent, and usually commences during puberty. MPHL presents as a progressive loss of scalp hair that follows a characteristic pattern. First, a bi-temporal recession of the hairline is noted. Then, the hair of the frontal and vertex areas of the scalp becomes thinner, leading to complete baldness of the top of the scalp (Blumeyer et al., 2011).

Specific pathophysiological features of MPHL are: (i) androgen dependency; (ii) the involvement of defined HF subpopulations of the scalp; (iii) a shortened anagen phase and premature entry into the catagen phase; and (iv) the transformation of terminal HF in vellus HF (Heilmann-Heimbach et al., 2016).

MPHL is a highly heritable polygenic disorder (Nyholt et al., 2003). To date, genome-wide association studies (GWAS) of MPHL have implicated more than 600 risk variants at more than 350 genomic loci (Yap et al., 2018). One of these loci implicates a region on chromosome 2, which contains single nucleotide variations (SNVs) that lead to a

downregulation of the expression of the gene *WNT10A* (wingless-type MMTV integration site family member 10A) (Hagenaars et al., 2017; Heilmann et al., 2013; Hochfeld et al., 2021; Pirastu et al., 2018; Yap et al., 2018). This gene codes for one of the mediators of the wnt pathway, WNT10A, which plays a fundamental role in the morphogenesis of all ectodermal appendages (skin, teeth, nails, and hair). Rare causal *WNT10A* biallelic pathogenic variants have been reported in two severe forms of ectodermal dysplasia (ED) and in non-syndromic tooth agenesis (Doolan et al., 2021). In human hair, *WNT10A* is expressed in the outer and inner root sheath and in hair shaft keratinocytes (Hochfeld et al., 2021). Since *WNT10A* is upregulated in human epithelial HF stem cells during the early anagen phase of the HF cycle, it is thought to play a role in HF anagen induction (Hawkshaw et al., 2020; Xu et al., 2017). Previous authors have therefore hypothesised that the risk allele in this locus contributes to the characteristic reduced anagen length and premature catagen entry of MPHL-HFs (Heilmann et al., 2013).

2.3 Aims

The three studies described in the present thesis were designed to: i) discover novel genes with an association to hair abnormalities; ii) identify novel pathogenic variants with an association to hair disorders; and iii) improve understanding of genotype-phenotype correlations of pathogenic variants implicated in hair disease. By characterising known and novel genes implicated in hair growth, we aimed to deepen understanding of HF biology. This in turn will pave the way for the development of new therapies.

2.4 References

Besnard T, Sloboda N, Goldenberg A, Kury S, Cogne B, Breheret F, Trochu E, Conrad S, Vincent M, Deb W, Balguerie X, Barbarot S, Baujat G, Ben-Omran T, Bursztejn AC, Carmignac V, Datta AN, Delignieres A, Faivre L, Gardie B, Gueant JL, Kuentz P, Lenglet M, Nassogne MC, Ramaekers V, Schnur RE, Si Y, Torti E, Thevenon J, Vabres P, Van Maldergem L, Wand D, Wiedemann A, Cariou B, Redon R, Lamaziere A, Bezieau S, Feillet F, Isidor B. Biallelic pathogenic variants in the lanosterol synthase gene LSS involved in the cholesterol biosynthesis cause alopecia with intellectual disability, a rare recessive neuroectodermal syndrome. Genet Med. 2019; 21: 2025-2035

Betz RC, Petukhova L, Ripke S, Huang H, Menelaou A, Redler S, Becker T, Heilmann S, Yamany T, Duvic M, Hordinsky M, Norris D, Price VH, Mackay-Wiggan J, de Jong A, DeStefano GM, Moebus S, Bohm M, Blume-Peytavi U, Wolff H, Lutz G, Kruse R, Bian L, Amos CI, Lee A, Gregersen PK, Blaumeiser B, Altshuler D, Clynes R, de Bakker PIW, Nothen MM, Daly MJ, Christiano AM. Genome-wide meta-analysis in alopecia areata resolves HLA associations and reveals two new susceptibility loci. Nat Commun. 2015; 6: 5966

Blumeyer A, Tosti A, Messenger A, Reygagne P, Del Marmol V, Spuls PI, Trakatelli M, Finner A, Kiesewetter F, Trueb R, Rzany B, Blume-Peytavi U, European Dermatology F. Evidence-based (S3) guideline for the treatment of androgenetic alopecia in women and in men. J Dtsch Dermatol Ges. 2011; 9 Suppl 6: S1-57

Doolan BJ, Onoufriadis A, Kantaputra P, McGrath JA. WNT10A, dermatology and dentistry. Br J Dermatol. 2021; 185: 1105-1111

Duverger O, Morasso MI. To grow or not to grow: hair morphogenesis and human genetic hair disorders. Semin Cell Dev Biol. 2014; 25-26: 22-33

Hagenaars SP, Hill WD, Harris SE, Ritchie SJ, Davies G, Liewald DC, Gale CR, Porteous DJ, Deary IJ, Marioni RE. Genetic prediction of male pattern baldness. PLoS genet. 2017; 13: e1006594

Hawkshaw NJ, Hardman JA, Alam M, Jimenez F, Paus R. Deciphering the molecular morphology of the human hair cycle: Wnt signalling during the telogen-anagen transformation. Br J Dermatol. 2020; 182: 1184–1193

Heilmann-Heimbach S, Hochfeld LM, Paus R, Nöthen MM. Hunting the genes in male-pattern alopecia: how important are they, how close are we and what will they tell us? Exp Dermatol. 2016; 25: 251–257

Heilmann S, Kiefer AK, Fricker N, Drichel D, Hillmer AM, Herold C, Tung JY, Eriksson N, Redler S, Betz RC, Li R, Kárason A, Nyholt DR, Song K, Vermeulen SH, Kanoni S, Dedoussis G, Martin NG, Kiemeney LA, Mooser V, Stefansson K, Richards JB, Becker T, Brockschmidt FF, Hinds DA, Nöthen MM. Androgenetic alopecia: identification of four genetic risk loci and evidence for the contribution of WNT signaling to its etiology. J Invest Dermatol. 2013; 133: 1489–1496

Hochfeld LM, Bertolini M, Broadley D, Botchkareva NV, Betz RC, Schoch S, Nothen MM, Heilmann-Heimbach S. Evidence for a functional interaction of WNT10A and EBF1 in male-pattern baldness. PLoS One. 2021; 16: e0256846

Lin X, Zhu L, He J. Morphogenesis, Growth Cycle and Molecular Regulation of Hair Follicles. Front Cell Dev Biol. 2022; 10: 899095

Millar SE. Molecular mechanisms regulating hair follicle development. J Invest Dermatol. 2002; 118: 216-225

Nyholt DR, Gillespie NA, Heath AC, Martin NG. Genetic basis of male pattern baldness. J Invest Dermatol. 2003; 121: 1561-1564

Oberlin KE, Maddy AJ, Martinez-Velasco MA, Vazquez-Herrera NE, Schachner LA, Tosti A. Short anagen syndrome: Case series and literature review. Pediatr Dermatol. 2018; 35: 388-391

Paus R, Cotsarelis G. The biology of hair follicles. N Engl J Med. 1999; 341: 491-497

Paus R, Muller-Rover S, Van Der Veen C, Maurer M, Eichmuller S, Ling G, Hofmann U, Foitzik K, Mecklenburg L, Handjiski B. A comprehensive guide for the recognition and classification of distinct stages of hair follicle morphogenesis. J Invest Dermatol. 1999; 113: 523-532

Pirastu N, Joshi PK, Vries PSd, Cornelis MC, McKeigue PM, Keum N, Franceschini N, Colombo M, Giovannucci EL, Spiliopoulou A, Franke L, North KE, Kraft P, Morrison AC, Esko T, Wilson JF. Author Correction: GWAS for male-pattern baldness identifies 71 susceptibility loci explaining 38% of the risk. Nat Commun. 2018; 9: 2536

Randolph MJ, Gwillim EC, Nguyen B, Tosti A. The psychologic impact of loose anagen syndrome and short anagen syndrome. Pediatr Dermatol. 2022; 39: 567-569

Rishikaysh P, Dev K, Diaz D, Qureshi WM, Filip S, Mokry J. Signaling involved in hair follicle morphogenesis and development. Int J Mol Sci. 2014; 15: 1647-1670

Romano M-T, Tafazzoli A, Mattern M, Sivalingam S, Wolf S, Rupp A, Thiele H, Altmüller J, Nürnberg P, Ellwanger J, Gambon R, Baumer A, Kohlschmidt N, Metze D, Holdenrieder S, Paus R, Lütjohann D, Frank J, Geyer M, Bertolini M, Kokordelis P, Betz RC. Bi-allelic Mutations in LSS, Encoding Lanosterol Synthase, Cause Autosomal-Recessive Hypotrichosis Simplex. Am J Hum Genet. 2018; 103: 777–785

Saxena N, Mok KW, Rendl M. An updated classification of hair follicle morphogenesis. Exp Dermatol. 2019; 28: 332-344

Schneider MR, Schmidt-Ullrich R, Paus R. The Hair Follicle as a Dynamic Miniorgan. Curr Biol. 2009; 19: R132-R142

Toussi A, Barton VR, Le ST, Agbai ON, Kiuru M. Psychosocial and psychiatric comorbidities and health-related quality of life in alopecia areata: A systematic review. J Am Acad Dermatol. 2021; 85: 162-175

Ü Basmanav FB, Cau L, Tafazzoli A, Méchin M-C, Wolf S, Romano MT, Valentin F, Wiegmann H, Huchenq A, Kandil R, Garcia Bartels N, Kilic A, George S, Ralser DJ, Bergner S, Ferguson DJP, Oprisoreanu A-M, Wehner M, Thiele H, Altmüller J, Nürnberg P, Swan D, Houniet D, Büchner A, Weibel L, Wagner N, Grimalt R, Bygum A, Serre G, Blume-Peytavi U, Sprecher E, Schoch S, Oji V, Hamm H, Farrant P, Simon M, Betz RC. Mutations in Three Genes Encoding Proteins Involved in Hair Shaft Formation Cause Uncombable Hair Syndrome. Am J Hum Genet. 2016; 99: 1292–1304

Xu M, Horrell J, Snitow M, Cui J, Gochnauer H, Syrett CM, Kallish S, Seykora JT, Liu F, Gaillard D, Katz JP, Kaestner KH, Levin B, Mansfield C, Douglas JE, Cowart BJ, Tordoff M, Liu F, Zhu X, Barlow LA, Rubin AI, McGrath JA, Morrisey EE, Chu EY, Millar SE. WNT10A mutation causes ectodermal dysplasia by impairing progenitor cell proliferation and KLF4-mediated differentiation. Nat Commun. 2017; 8: 15397

Yang F, Jiang X, Zhu Y, Lee M, Xu Z, Zhang J, Li Q, Lin MY, Wang H, Lin Z. Biallelic Variants in Lanosterol Synthase (LSS) Cause Palmoplantar Keratoderma-Congenital Alopecia Syndrome Type 2. J Invest Dermatol. 2022; 142: 2687-2694 e2682

Yap CX, Sidorenko J, Wu Y, Kemper KE, Yang J, Wray NR, Robinson MR, Visscher PM. Dissection of genetic variation and evidence for pleiotropy in male pattern baldness. Nat Commun. 2018; 9: 5407

Zhao L, Chen XJ, Zhu J, Xi YB, Yang X, Hu LD, Ouyang H, Patel SH, Jin X, Lin D, Wu F, Flagg K, Cai H, Li G, Cao G, Lin Y, Chen D, Wen C, Chung C, Wang Y, Qiu A, Yeh E, Wang W, Hu X, Grob S, Abagyan R, Su Z, Tjondro HC, Zhao XJ, Luo H, Hou R, Jefferson J, Perry P, Gao W, Kozak I, Granet D, Li Y, Sun X, Wang J, Zhang L, Liu Y, Yan YB, Zhang K. Lanosterol reverses protein aggregation in cataracts. Nature. 2015; 523: 607-611

Zhou S, Jiang X, Zhu Y, Yang J, Yuan C, Chen M, Zhou Q, Lin Z, Li M. Biallelic mutations in LSS in autosomal-recessive mutilating palmoplantar keratoderma. Exp Dermatol. 2023; 32: 699-706

3. Publications

3.1 Publication 1:

Cesarato N, Schwieger-Briel A, Gossmann Y, Henne SK, Hillmann K, Frommherz LH, Wehner M, Xiong X, Thiele H, Oji V, Milani D, Tantcheva-Poor I, Giehl K, Folster-Holst R, Teichler A, Braeckmans D, Hoeger PH, Jones G, Frank J, Weibel L, Blume-Peytavi U, Hamm H, Nothen MM, Geyer M, Heilmann-Heimbach S, Basmanav FB, Betz RC. Short anagen hair syndrome: Association with mono- and biallelic variants in WNT10A and a genetic overlap with male pattern hair loss. Br J Dermatol. 2023;

Br J Dermatol 2023; **00**:1–9
https://doi.org/10.1093/bjd/ljad314
Advance access publication date: 6 September 2023

BJD
British Journal of Dermatology
Translational Research

Short anagen hair syndrome: association with mono- and biallelic variants in *WNT10A* and a genetic overlap with male pattern hair loss

Nicole Cesarato,[1] Agnes Schwieger-Briel,[2,3] Yasmina Gossmann,[1] Sabrina K. Henne,[1] Kathrin Hillmann,[4] Leonie H. Frommherz,[5] Maria Wehner,[1] Xing Xiong,[1] Holger Thiele,[6] Vinzenz Oji,[7] Donatella Milani,[8] Iliana Tantcheva-Poor,[9] Kathrin Giehl,[5] Regina Fölster-Holst,[10] Anne Teichler,[11] Delphine Braeckmans,[11] Peter H. Hoeger,[11] Gabriela Jones,[12] Jorge Frank,[13] Lisa Weibel,[2] Ulrike Blume-Peytavi,[4] Henning Hamm,[14] Markus M. Nöthen,[1] Matthias Geyer,[15] Stefanie Heilmann-Heimbach,[1] F. Buket Basmanav[1] and Regina C. Betz[1]

[1]Institute of Human Genetics and [15]Institute of Structural Biology, University of Bonn, Medical Faculty and University Hospital Bonn, Bonn, Germany
[2]Department of Pediatric Dermatology, University Children's Hospital Zurich, Zurich, Switzerland
[3]Department of Dermatology, Medical Center – University of Freiburg, Freiburg, Germany
[4]Department of Dermatology, Venereology and Allergology, Charité – Universitätsmedizin Berlin, Berlin, Germany
[5]Department of Dermatology and Allergy, Ludwig-Maximilian-University of Munich, Munich, Germany
[6]Cologne Center for Genomics, University of Cologne, Cologne, Germany
[7]Department of Dermatology, University Hospital of Muenster, Muenster, Germany
[8]Fondazione IRCCS Ca' Granda Ospedale Maggiore Policlinico, Milan, Italy
[9]Department of Dermatology, Faculty of Medicine and University Hospital Cologne, University of Cologne, Cologne, Germany
[10]Department of Dermatology, Venereology and Allergology, University Hospital Schleswig-Holstein, Kiel, Germany
[11]Department of Paediatric Dermatology, Catholic Children's Hospital Wilhelmstift, Hamburg, Germany
[12]Clinical Genetics Department, Nottingham University Hospitals NHS Trust, Nottingham, UK
[13]Department of Dermatology, Venereology and Allergology, University Medical Center Göttingen, Göttingen, Germany
[14]Department of Dermatology, Venereology, and Allergology, University Hospital Würzburg, Würzburg, Germany

N.C. and A.S.-B. contributed equally to this work and are joint first authors.

Correspondence: Regina C. Betz. Email: regina.betz@uni-bonn.de

Abstract

Background Short anagen hair (SAH) is a rare paediatric hair disorder characterized by a short anagen phase, an inability to grow long scalp hair and a negative psychological impact. The genetic basis of SAH is currently unknown.

Objectives To perform molecular genetic investigations in 48 individuals with a clinical phenotype suggestive of SAH to identify, if any, the genetic basis of this condition.

Methods Exome sequencing was performed in 27 patients diagnosed with SAH or with a complaint of short, nongrowing hair. The cohort was screened for variants with a minor allele frequency (MAF) < 5% in the general population and a Combined Annotation Dependent Depletion (CADD) score > 15, to identify genes whose variants were enriched in this cohort. Sanger sequencing was used for variant validation and screening of 21 additional individuals with the same clinical diagnosis and their relatives. Genetic association testing of SAH-related variants for male pattern hair loss (MPHL) was performed using UK Biobank data.

Results Analyses revealed that 20 individuals (42%) carried mono- or biallelic pathogenic variants in *WNT10A*. Rare *WNT10A* variants are associated with a phenotypic spectrum ranging from no clinical signs to severe ectodermal dysplasia. A significant association was found between *WNT10A* and SAH, and this was mostly observed in individuals with light-coloured hair and regression of the frontoparietal hairline. Notably, the most frequent variant in the cohort [c.682T>A;p.(Phe228Ile)] was in linkage disequilibrium with four common *WNT10A* variants, all of which have a known association with MPHL. Using UK Biobank data, our analyses showed that c.682T>A;p.(Phe228Ile) and one other variant identified in the SAH cohort are also associated with MPHL, and partially explain the known associations between *WNT10A* and MPHL.

Conclusions Our results suggest that *WNT10A* is associated with SAH and that SAH has a genetic overlap with the common phenotype MPHL. The presumed shared biologic effect of *WNT10A* variants in SAH and MPHL is a shortening of the anagen phase. Other factors, such as modifier genes and sex, may also play a role in the clinical manifestation of hair phenotypes associated with the *WNT10A* locus.

Accepted: 23 August 2023
© The Author(s) 2023. Published by Oxford University Press on behalf of British Association of Dermatologists. All rights reserved. For permissions, please e-mail: journals.permissions@oup.com

What is already known about this topic?

- Short anagen hair (SAH) is a hair anomaly characterized by short, nongrowing hair. To date, no genetic cause for SAH has been described.
- Although *WNT10A* is associated with ectodermal dysplasia (ED), mutation carriers do not necessarily present with the full clinical picture of ED and some present with hair anomalies. However, no isolated hair phenotype occurring in association with rare *WNT10A* variants has yet been reported.

What does this study add?

- We genetically investigated 48 individuals, mostly girls clinically diagnosed with SAH or with the complaint of short, nongrowing hair; in 40% of these patients, we identified bi- or monoallelic pathogenic variants in *WNT10A*.
- We showed that two of these variants are also associated with male pattern hair loss (MPHL).
- Notably, clinical examination of the *WNT10A*-related SAH phenotype revealed light-coloured, poorly growing hair and a high/receding hairline in most girls.

What is the translational message?

- SAH is associated with rare or low-frequency variants in *WNT10A*.
- Clinically, individuals with SAH who carry *WNT10A* variants tend to show a bilateral frontoparietal recession of the hairline and nongrowing hair in early childhood.
- Molecular analysis of *WNT10A* can confirm the clinical diagnosis of SAH.
- The presumed shared biologic effect of *WNT10A* variants in SAH and MPHL is a shortening of the anagen phase of the hair follicle.

Short anagen hair (SAH) is an isolated hair abnormality characterized by the inability to grow long scalp hair. SAH was first described in the 1990s.[1,2] The majority of reported patients with SAH were aged 3–6 years and have been female.[3] Although SAH is regarded as a rare condition, its exact prevalence remains unknown.

Particularly in early childhood, SAH hair is fine and has a low-to-normal density. Hair length is restricted to around 3–10 cm, primarily attributable to a shortened anagen phase.[3] The anagen : telogen ratio is shifted from around 9 : 1 to 2 : 1.[4] Correspondingly, the hair-pull test is often positive, although this is not pronounced.[5,6] Hair shafts have a normal anatomy with tapered ends,[5] as is typical for uncut hair, and are of variable diameter.[4] Although rarely performed, scalp biopsies show terminal and vellus hair follicles with mild lymphocytic infiltrates.[7] In many cases, the SAH phenotype improves with age and may resolve spontaneously during puberty. Research suggests that SAH has a negative emotional, psychological and social impact on both affected children and their parents.[8]

To date, few data are available on the genetic aetiology of SAH. Most reported cases have been sporadic, although familial cases have also been described.[2] The aim of the current study was to investigate, if any, the genetic basis of SAH in a cohort of individuals ($n=48$), all of whom had sought medical consultation with the complaint of lack of hair length (SAH cohort).

Investigation of the present cohort revealed the presence of pathogenic variants in *WNT10A* in 42% of the individuals and a typical *WNT10A*-associated hair phenotype. We also report that two of the SAH variants are significantly associated with the risk of developing male pattern hair loss (MPHL) and are partially responsible for the previously known associations between the *WNT10A* locus and MPHL.[9–13]

Patients and methods

Study participants

The present cohort comprised 48 individuals (45 females, 3 males) who were referred to us with either a clinical diagnosis of SAH ($n=36$) or a clinical phenotype suggestive of SAH (short, nongrowing hair; $n=12$) [Figure 1, Appendix S1 (see Supporting Information)]. When possible, DNA was also collected from the respective parents.

Sequencing

The DNA of 27 individuals (25 females, 2 males) was subjected to whole-exome sequencing (WES) at the Cologne Center for Genomics (Cologne, Germany), as described elsewhere.[14] Polyphen and Combined Annotation Dependent Depletion (CADD) were used to predict the pathogenicity of the variants.[15,16] WES data were filtered to identify genes for which at least 20% of the cohort ($n=5$) carried rare variants [minor allele frequency (MAF) $<1\%$]. Following the lack of evidence for any plausible genes, we changed the MAF to $<5\%$ and used a CADD score >15. WES result verification, co-segregation analysis, targeted *WNT10A* screening in additional 21 affected individuals (20 females, 1 male) and genotyping of single nucleotide polymorphisms (SNPs) with a reported association with MPHL were performed using Sanger sequencing with the BigDye Terminator v1.1 Cycle Sequencing Kit (Applied Biosystems, Foster City, CA, USA) and an ABI 3100 genetic analyser (Applied Biosystems).

Bioinformatic analysis

Statistical analyses were performed using R version 4.1.2 (https://www.r-project.org/).[17] Data from individuals of

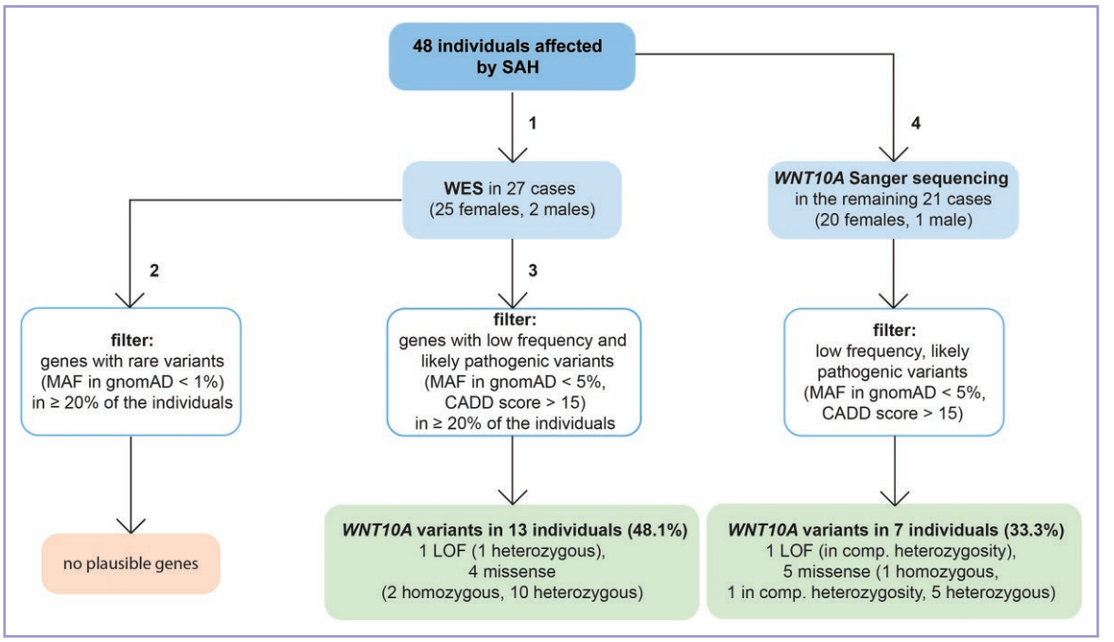

Figure 1 Study design and results obtained in the short anagen hair (SAH) cohort. The DNA of 27 affected individuals was subjected to whole-exome sequencing (WES) (1). In cases that underwent WES, we initially did not identify any plausible genes after filtering of the data for rare variants [minor allele frequency (MAF) < 1%] that affect a common gene in at least 20% of the cohort (5 individuals) (2). However, an enrichment was observed in *WNT10A* when the criteria for qualifying variants was adjusted to an MAF < 5% and a Combined Annotation Dependent Depletion (CADD) score > 15 (3). Here, 13 of 27 individuals (48%) carrying heterozygous or homozygous loss of function (LOF) or missense variants in *WNT10A*. *WNT10A* sequencing in the remaining 21 individuals (4) confirmed the results obtained in the WES cohort, with 7 affected individuals being found to carry *WNT10A* variants.

non-Finnish European ancestry ($n = 67\,942$ alleles) from the gnomAD database were used to calculate the frequency of likely pathogenic *WNT10A* variants in the population and for the enrichment analysis, as detailed in Appendix S2 (see Supporting Information).[18] Data were analysed using Fisher's exact test (two-tailed) with a 95% confidence interval. CADD scores were obtained from https://cadd.gs.washington.edu (version 1.6).[15] Haplotype data were retrieved from the online LDhap Tool (https://ldlink.nci.nih.gov/?tab=ldhap).[19]

Modelling of *WNT10A* mutations

Two structural models of human Wnt family member 10A (*WNT10A*) were generated using the SWISS-MODEL workspace approach.[20] The first model was based on the 2.8 Å resolution crystal structure of human Wnt family member 3 (WNT3) in complex with the mouse Frizzled-8 Cys-rich domain [CRD; Protein Data Bank (PDB) accession code 6AHY].[21] The second model was based on the 2.2 Å resolution cryo-electron microscopy structure of human Wnt family member 3A (WNT3A) in complex with Wntless (PDB accession code 7DRT).[22] Both models are in good agreement with the AlphaFold2 structure prediction of human *WNT10A* (Appendix S3; see Supporting Information).[23]

Association between short anagen hair-related *WNT10A* variants and male pattern hair loss

A total of 72 024 male participants of the UK Biobank 200k exome release were selected based on their self-reported MPHL status. These were stratified as cases and controls, as described in Figure S1 (see Supporting Information), and their WES and genotyping data were downloaded from the UK Biobank in PLINK format and filtered for *WNT10A* variants (gene boundaries ± 30 kb). Single-variant analyses of exome and genotype data were performed in PLINK 2.0 using the *glm* function,[24] with age and the top 14 principal components as covariates. Summary statistics were then combined and prepared for fine-mapping using the PolyFun *munge_polyfun_sumstats* script.[25] Fine-mapping of summary statistics was performed with the SuSiE method in the PolyFun *finemapper* wrapper,[26,27] using precomputed summary linkage disequilibrium information from the UK Biobank (https://registry.opendata.aws/ukbb-ld/?/, accessed 14 November 2022) and the *max-num-causal 10* and *allow-missing* parameters.

Results

Sequencing revealed mono- and biallelic *WNT10A* variants in the short anagen hair cohort

Analysis of the WES data for the presence of likely pathogenic variants revealed that 13 affected individuals (12 females, 1 male) of 27 (48%) carried missense or loss-of-function (LOF) variants in *WNT10A*, in either a homozygous (2 individuals) or a heterozygous state (11 individuals). Sanger sequencing of *WNT10A* in the remaining 21 individuals revealed seven other females (33%) who presented with mono- ($n = 5$) or biallelic ($n = 2$) LOF or missense variants (Figure 1).

The most common variant in our entire cohort was c.682T>A;p.(Phe228Ile). The status of this variant (heterozygous, homozygous or compound heterozygous) and all other variants are provided in Table 1 and Table S1 (see Supporting Information). One female carried the variants c.682T>A;p.(Phe228Ile) and c.934C>A;p.(Pro312Thr) on the same maternally inherited allele (Table 1, Table S1). In total, qualifying *WNT10A* variants were identified in 42% of the individuals in the present cohort [Table 1; Figure S2, Tables S1, S2 (see Supporting Information)].

Enrichment of *WNT10A* variants in the short anagen hair cohort vs. the general population

The overall allele frequency of likely pathogenic *WNT10A* variants in the control cohort from the gnomAD database was 0.04. With an overall allele frequency of 0.25, the overall burden of *WNT10A* variants in the present SAH cohort was significantly higher compared with the control cohort ($P = 5.033 \times 10^{-12}$, Fisher's exact test) (Table 2).

For each variant, the allele frequency was compared between the two cohorts (Table S3; see Supporting Information). Seven of the eight variants were either observed exclusively, or were significantly enriched, in the SAH cohort. Notably, the most commonly observed variant [i.e. c.682T>A;p.(Phe228Ile)] showed a nearly 10-fold enrichment in SAH vs. controls ($P = 5.191 \times 10^{-11}$, Fisher's exact test).

A second, more conservative burden analysis excluding c.682T>A;p.(Phe228Ile) also showed significant enrichment of *WNT10A* variants in SAH, confirming that c.682T>A;p.(Phe228Ile) is not the only pathogenic variant or the sole signal driver in the burden analysis (Table S4, Appendix S4; see Supporting Information).

WNT10A-associated hair phenotype in the short anagen hair cohort

Clinical photographs were available for 18 individuals with pathogenic *WNT10A* variants. The majority of these individuals presented with sparse, light-coloured hair and a high frontal hairline with bilateral frontoparietal recession (Figure 2). In almost all cases, the hair grew longer in the temporal and occipital areas of the scalp than in the frontal area (average difference of around 5–10 cm). The affected individuals had never needed a haircut. Results of the hair-pull test were available for 11 cases; in 9 cases, the result was negative (Table S5; see Supporting Information).

Short anagen hair-associated variants have reduced penetrance and mild effects on other ectodermal tissues

Biallelic *WNT10A* variants are known to cause ectodermal dysplasia (ED).[28] Furthermore, many reports describe mono- or biallelic *WNT10A* variants for nonsyndromic tooth agenesis (NSTA) with reduced penetrance.[29] Therefore, we sequenced the variants identified in the individuals affected by SAH in their respective parents or siblings (28 individuals from 14 families). Subsequently, patients with SAH with *WNT10A* variants were contacted again, to enquire about the presence of teeth and/or nail abnormalities, and of any history of hair, teeth and/or nail abnormalities in their parents or siblings. Self-reported information was received for 12 of the 20 individuals affected by SAH and 14 relatives with *WNT10A* variants (Table S5; see Supporting Information).

Three female individuals with SAH and biallelic variants reported teeth and/or nail involvement. For most of the

Table 1 *WNT10A* variants identified in the present short anagen hair cohort, as detected by whole-exome (WES) and/or Sanger sequencing

Allele 1	Allele 2	No. of individuals	Individual ID	Detection
c.321C>A;p.(Cys107*)	–	1	12	WES
c.321C>A;p.(Cys107*)	c.682T>A;p.(Phe228Ile)	1	17	Sanger
c.487C>T;p.(Arg163Trp)	–	1	15	Sanger
c.493G>A;p.(Gly165Arg)	–	1	20	Sanger
c.682T>A;p.(Phe228Ile)	–	9	1, 2, 4, 6, 7, 9, 10, 13, 19	WES, Sanger
c.682T>A;p.(Phe228Ile), c.934C>A;p.(Pro312Thr)	–	1	18	Sanger
c.682T>A;p.(Phe228Ile)	c.682T>A;p.(Phe228Ile)	3	5, 8, 16	WES, Sanger
c.688G>T;p.(Asp230Tyr)	–	1	14	WES
c.822G>C;p.(Lys274Asn)	–	1	3	WES
c.910A>C;p.(Asn304His)	–	1	11	WES

Table 2 Overall prevalence of *WNT10A* variants (minor allele frequency < 5%; Combined Annotation Dependent Depletion > 15) in the short anagen hair (SAH) cohort vs. the non-Finnish European gnomAD population

SAH cohort				Non-Finnish European gnomAD				
No. of variants	Allele count	Total allele count	Overall frequency	No. of variants	Allele count	Total allele count	Overall frequency	*P*-value
8	24	96	0.25	141	3042	67 942	0.04477	5.033×10^{-12}

In this analysis, the allele carrying both c.682T>A;p.(Phe228Ile) and c.934C>A;p.(Pro312Thr) was counted only once as an 'affected allele'.

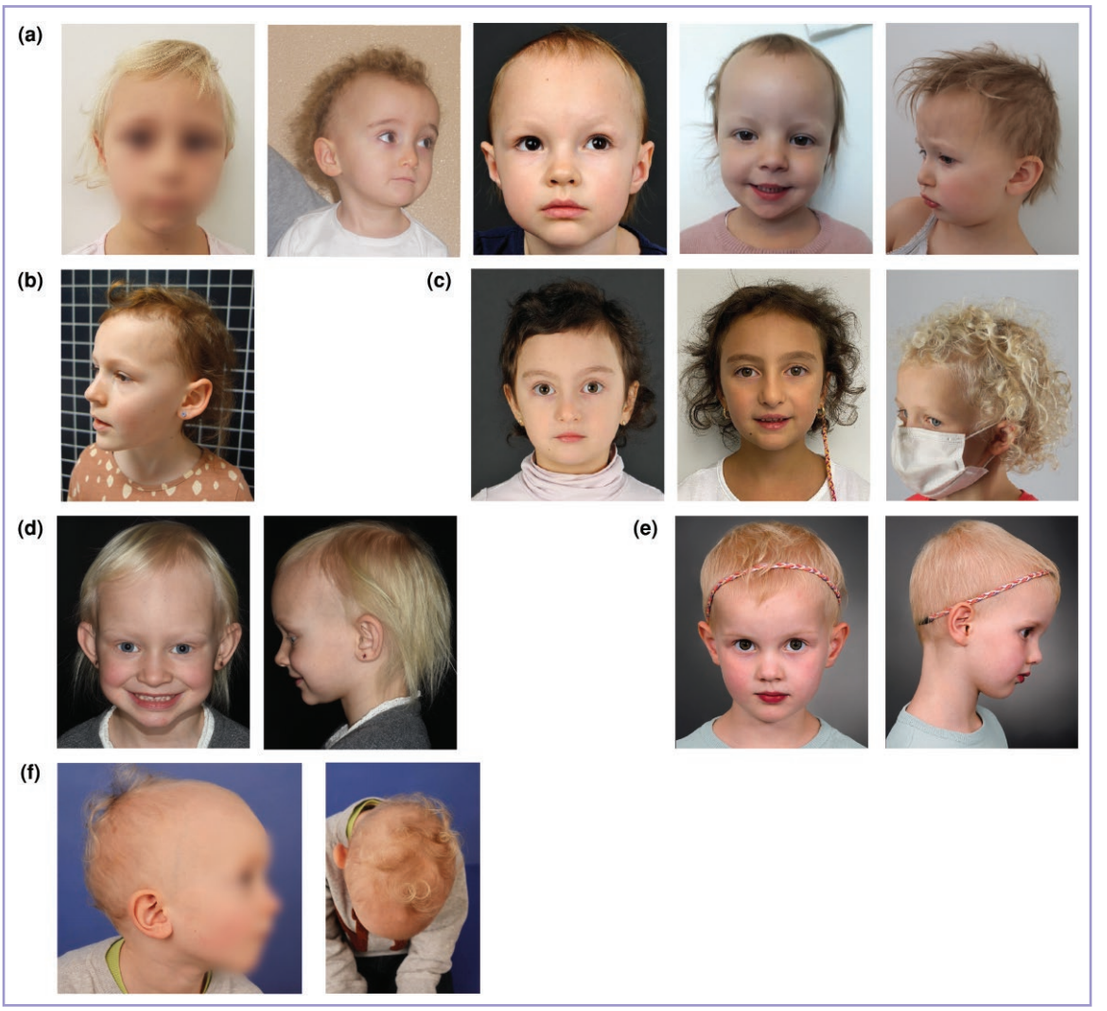

Figure 2 Clinical photographs of individuals with *WNT10A* variants from the short anagen hair cohort. (a) Individuals 4, 6, 9, 10 and 19 carried the variant c.682T>A;p.(Phe228Ile) in a heterozygous state. (b) Individual 18 carried the variants c.682T>A;p.(Phe228Ile) and c.934C>A;p.(Pro312Thr) in a heterozygous state on the same allele. (c) Individual 8, at the age of 5 and 7 years, and individual 16, both of whom carried the variant c.682T>A;p.(Phe228Ile) in a homozygous state. (d) Individual 15 carried the variant c.487C>T;p.(Arg163Trp) in a heterozygous state (frontal and lateral views). (e) Individual 11 carried the variant c.910A>C;p.(Asn304His) in a heterozygous state (frontal and lateral views). (f) Individual 3 (the only male variant carrier in the cohort) carried the variant c.822G>C;p.(Lys274Asn) in a heterozygous state (lateral and superior views).

SAH cases who carried monoallelic variants, no or only very mild additional features were reported. Of the 14 relatives with *WNT10A* monoallelic variants, three mothers (21%) described the presence of fine or low-density hair and 11 (79%) relatives reported no ectodermal features (Table S5).

Structural modelling of *WNT10A* mutant sites

WNT10A consists of the characteristic palm, thumb and index finger configuration (Figure 3a). A premature stop of Cys107 is likely to result in the abolition of *WNT10A* protein translation (Figure 3b). Phe228 of *WNT10A* is conserved in WNT3A and WNT8A, with its hydrophobic side chain being entirely buried in the assembly of a central six-helix bundle. Its mutation to a smaller isoleucine may induce the reassembly of the helices, leading to conformational changes of the central palm domain. Asp230, on the back of Phe228 within the same helix, is involved in a whole cluster of salt bridges interacting with Arg243, Arg248 and Arg251, as well as Leu244 of the following helix. The much larger tyrosine not only abrogates the charge-induced association with the arginines, but also hinders the tight assembly of these helices. Arg163 and Lys274 are at the interface to Wntless. The present analysis suggests that Arg163 exchange to tryptophan and Gly165 to arginine might lead to alterations in Wntless binding and the interaction with the lipid bilayer. The residue corresponding to Lys274 in WNT3A forms hydrogen bonds with one of the transmembrane helices in Wntless,[22] and is also in close proximity to the Frizzled-8 binding site of WNT3A (Figure S3b; see Supporting Information).[21] Finally, Asp304 and Pro312 are located opposite the Wntless/Frizzled-8 binding site of *WNT10A* on the periphery of the central six-helical bundle (Figure 3b). Mutation of these residues may induce conformational changes that lead to an

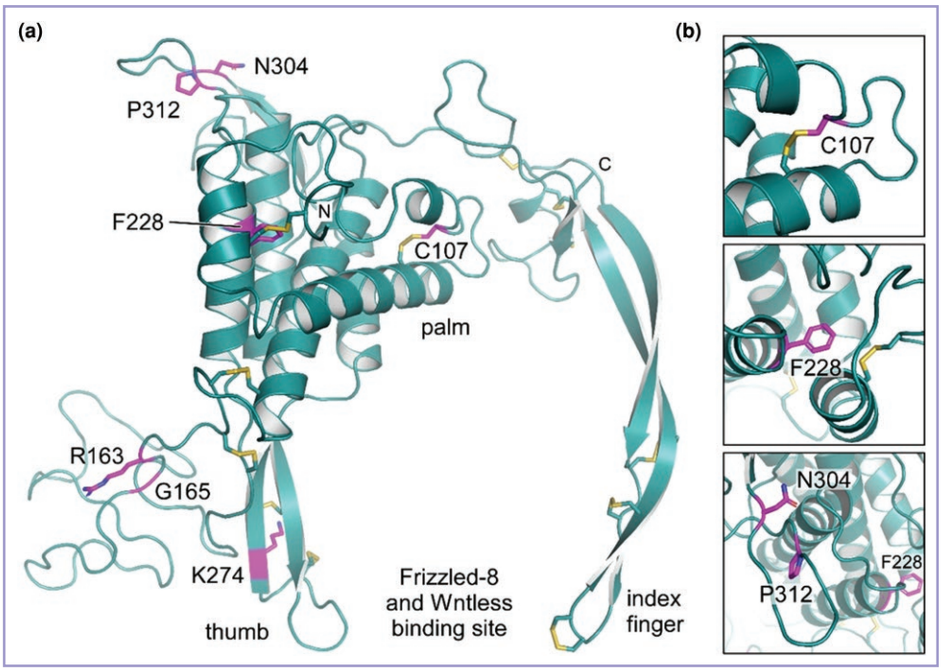

Figure 3 Depiction of the pathogenic variants in the structure of Wnt family member 10A (*WNT10A*). (a) Model of the structure of human *WNT10A*, based on the WNT3–Frizzled-8 crystal structure (Protein Data Bank 6ahy). The positions of the seven identified genetic variants are highlighted in magenta. The overall fold adopts the characteristic hand-like structure, with a central palm domain and two opposing β-hairpins, described as the thumb and index finger, involved in Frizzled and Wntless binding. The extracellular protein is stabilized by the formation of 12 intramolecular disulfide bonds. (b) Close-up of the interaction sites of residues Cys107 (top), Phe228 and Asp230 (middle), and the dual sites Asn304 and Pro312 (bottom).

Table 3 Frequencies of all haplotypes encompassing the male pattern hair loss single nucleotide polymorphisms and rs121908120 [c.682T>A; p.(Phe228Ile)] in the non-Finnish European population retrieved from the LDhap Tool

rs3856551		rs74333950		rs121908120		rs7349332		rs77157375		Haplotype count	Haplotype frequency
C=0.887	T=0.113	T=0.881	G=0.119	T=0.978	A=0.022	C=0.889	T=0.111	G=0.968	A=0.032		
C		T		T		C		G		711	0.88
T		G		T		T		G		64	0.0792
T		**G**		**A**		**T**		**A**		**17**	**0.021**
T		G		T		T		A		8	0.0099
C		G		T		C		G		5	0.0062
C		T		T		C		A		1	0.0012
T		G		A		T		G		1	0.0012
T		G		T		C		G		1	0.0012

Male pattern hair loss risk alleles are highlighted in orange. The short anagen hair-associated variant c.682T>A is highlighted in yellow. The most prevalent haplotype observed in the present cohort is indicated in bold.

alteration in protein function or may affect interaction with other binding partners.[30]

Genetic overlap between short anagen hair and male pattern hair loss over the *WNT10A* locus

Five SNPs located within, or in the vicinity of, *WNT10A* have a reported association with MPHL (rs3856551,[9] rs74333950,[10] rs7349332,[10–12] rs77157375,[12] rs192913879[13]). As a shortening of the anagen phase is a pathophysiological feature of both MPHL and SAH, sequencing of the MPHL-associated SNPs was performed in *WNT10A* variant carriers from the present cohort (Table S1; see Supporting Information). All individuals and parents with the c.682T>A;p.(Phe228Ile) variant were found to carry the MPHL-associated risk alleles of the SNPs rs3856551, rs74333950, rs7349332 and rs77157375, suggesting genetic linkage between these markers. The LDhap Tool confirmed this,[19] and suggested that c.682T>A;p.(Phe228Ile) arose on a low-frequency haplotype block containing the risk alleles of the four MPHL-associated SNPs (Table 3).

Accordingly, analyses were performed to determine whether c.682T>A;p.(Phe228Ile) and other SAH-related variants identified in the present cohort are associated with MPHL using the data of 72 024 males from the UK Biobank cohort. MPHL status was defined using two models (i.e. regular and two-as-control; Figure S1 (see Supporting Information). Both models showed that c.682T>A;p.(Phe228Ile) and c.321C>A;p.(Cys107*) were significantly associated with MPHL (Table S6; see Supporting

Information). Fine-mapping analysis was performed to determine whether these two *WNT10A* variants explain the previously reported associations between common variants at the *WNT10A* locus and MPHL. The results revealed two and three 95% credible SNP sets for the regular model and the two-as-control model, respectively (Table S7; see Supporting Information). While the association signal in the former was mainly explained by the low-frequency variant c.682T>A;p.(Phe228Ile) [posterior inclusion probability (PIP) = 0.983] and the common variants rs7349332 (PIP = 0.715) and rs10177996 (PIP = 0.285), the association signal in the latter was additionally explained by the rare variant c.321C>A;p.(Cys107*) (PIP = 0.995).

Discussion

Rare biallelic variants in *WNT10A* have been associated with diverse forms of ED, including Schöpf–Schulz–Passarge syndrome (MIM 224750), odonto-onychodermal dysplasia (MIM 257980) and hypohidrotic and anhidrotic ectodermal dysplasia.[29,31,32] Mono- and biallelic *WNT10A* variants have also been identified in NSTA (MIM 150400).[29,33] Indeed, monoallelic *WNT10A* variants are associated with a highly variable phenotypic spectrum, ranging from no clinical signs to ED.[29,34] A genetic study suggested that heterozygous carriers of pathogenic *WNT10A* variants (mostly captured as the parents of index cases with ED or NSTA) might show minor anomalies/impairments of one or more ectodermal derivatives with a sex-biased manifestation pattern. While female patients were more likely to display hair or nail phenotypes, male patients tended to present with teeth defects.[28] This was supported by a recent meta-analysis of 287 articles on *WNT10A* variants and genetic diagnoses.[29] In both mono- and biallelic *WNT10A* cases reported to date, teeth involvement has been a major focus of attention. In contrast, hair-related phenotypes have not been subjected to in-depth analysis, although a disturbance of hair growth (i.e. thin/fragile/sparse/thick scalp/body hair, hypotrichosis or alopecia)[28,29,34] was observed in 90% and 33% of biallelic and monoallelic *WNT10A* cases with a clinical diagnosis, respectively.[29] In five biallelic cases from the literature, 'slow-growing' hair was also reported.[34–36]

The present report relates low-frequency and rare genetic variants in *WNT10A* to a distinct hair phenotype with a clinical diagnosis, namely SAH. Based on the few reports that mention slow-growing hair as a symptom of *WNT10A*-associated ED and our own observation of teeth abnormalities in three of the four biallelic *WNT10A* variant carriers in the present cohort, we propose that SAH can present as (i) an additional and under-recognized feature of *WNT10A*-associated ED, which mainly affects biallelic carriers; or (ii) an isolated phenotype, which mainly affects female heterozygous carriers. Therefore, *WNT10A* variants should be considered causative for SAH with reduced penetrance and variable expressivity. In this sense, the genomic context (e.g. common genetic variations, modifier genes and epigenetic factors), sex and other environmental factors are expected to be determinants of whether – and to what extent – a (hair) phenotype is manifested. A plausible hypothesis is that other causal genes exist, thus pointing to genetic heterogeneity, and that these genes explain the SAH phenotype in the remaining patients. Notably, a similar autosomal dominant mode of inheritance with reduced penetrance and variable expressivity has also been described for *WNT10A*-associated NSTA.[28,29]

Importantly, most individuals with *WNT10A*-related SAH in the present cohort presented with light-coloured hair, which was generally longer in the occipital and temporal regions of the scalp than in the frontal region, and with a bilateral frontoparietal recession of the hairline. To some extent, the latter feature resembles early signs of MPHL.

The present SAH cohort was mainly composed of girls. This could be attributable to the fact that a short hair phenotype may remain undiagnosed in boys, who typically opt for shorter hairstyles. An alternative potential explanation is that the majority of male heterozygous *WNT10A* carriers do not manifest a hair phenotype, owing to the previously reported sex-dependent effects of *WNT10A* variants.[28,29]

In the present cohort, c.682T>A;p.(Phe228Ile) was identified in more than every third affected girl. In the (non-Finnish) European population (gnomAD), this variant has a MAF of around 2%. In contrast, the MAF of this variant in the present SAH cohort, which mostly comprised individuals of European origin, is 18%. In the literature, c.682T>A;p.(Phe228Ile) has already been described in association with teeth anomalies and with ED.[28,29] Despite its high prevalence in our SAH cohort, several explanations can be proposed as to why the association between c.682T>A;p.(Phe228Ile) and SAH has remained unrecognized to date. These include reduced penetrance and variable expressivity, and the possibility that SAH is underdiagnosed, especially when present as an isolated phenotype. With respect to the other variants of possible causal relevance, each was observed in one or a maximum of two affected individuals, and thus their association with SAH remains uncertain. To determine their definite involvement, the investigation of larger numbers of affected individuals is required. However, the significant results of the burden analysis after removal of individuals with c.682T>A;p.(Phe228Ile) suggest that these variants include true causal mutations.

Notably, c.682T>A;p.(Phe228Ile) and one other variant observed in two cases from the present cohort [i.e. c.321C>A;p.(Cys107*)] also showed significant associations with the common phenotype MPHL, whose key pathophysiological features include changes in hair cycle dynamics (i.e. a shortening of the anagen phase and a prolongation of the catagen phase).[37] These findings, and the identification of a rare haplotype that contained c.682T>A;p.(Phe228Ile) and four common MPHL associated risk alleles, prompted the hypothesis that c.682T>A;p.(Phe228Ile) and/or c.321C>A;p.(Cys107*) may explain the association between *WNT10A* and MPHL. Our fine-mapping analyses showed that these variants are partially – although not entirely – responsible for the association between *WNT10A* and MPHL.

WNT10A is involved in the differentiation of hair, teeth, skin, sweat glands, tongue and nail tissues.[38] Research has shown that the Wnt pathway regulates the hair follicle (HF) cycle.[39,40] In mice, *Wnt10a* knockout causes altered hair cycle progression, with an acceleration of the catagen phase and a delay in anagen induction. The hair shafts of knockout mice are shorter and thinner than those of control mice, and

display a disorganized internal structure.[38] In humans, it has been demonstrated that *WNT10A* is upregulated in human epithelial HF stem cells during the early anagen phase of the HF cycle, a finding that supports its hypothesized role in anagen induction.[41] Research has shown that *WNT10A* is also expressed in the outer and inner root sheath and hair shaft keratinocytes of anagen and catagen HFs.[9] A previous immunohistochemical analysis of skin samples of individuals with biallelic *WNT10A* LOF variants [including the SAH-related c.321C>A;p.(Cys107*)] showed malformed HFs with disorderly differentiation and root sheath formation, which was accompanied by less pronounced *WNT10A* staining in comparison to control skin samples, which further supports the role of *WNT10A* in HF biology.[42] Interestingly, a recent study showed that the *WNT10A* p.(Phe228Ile) variant failed to activate the Wnt pathway in stem cells from human exfoliated deciduous teeth.[43] A reasonable hypothesis is that this and other missense variants identified in the present cohort have a similar effect on HF (stem) cells by inducing conformational changes, or by influencing the interactions of *WNT10A* with its binding partners, as suggested by the protein modelling.

At the time of writing, no curative therapies are available for SAH. However, oral biotin supplements, and biotin in association with topical minoxidil, may improve hair length and density.[4,44] Interestingly, minoxidil was proposed to prolong the anagen phase via the induction of β-catenin activity, a key component of the Wnt pathway, and is known to be beneficial in MPHL.[45,46]

In conclusion, this study underlines the involvement of *WNT10A* in both rare and common hair disorders, and describes a *WNT10A*-related hair phenotype that can be confirmed by molecular diagnostic screening of *WNT10A* in individuals with complaints suggestive of SAH, either as an isolated phenotype or in the presence of other ectodermal anomalies.

Acknowledgements

We thank the affected individuals and their families for their participation.

Funding sources

This work was supported by a grant from the German-Israeli Foundation for Scientific Research and Development (GIF) to R.C.B. and by the German Research Foundation (Deutsche Forschungsgemeinschaft, DFG), under the auspices of the German Excellence Strategy (EXC2151–390873048) to M.M.N. and R.C.B. X.X. received a scholarship from the China Scholarship Council (no. 202208080206).

Conflicts of interest

The authors declare no conflicts of interest.

Data availability

The data underlying this article are available upon reasonable request from the corresponding author.

Ethics statement

The study was performed in accordance with the principles of the Declaration of Helsinki. Ethical approval was obtained from the ethics committee of the Medical Faculty of the University of Bonn. All participants or legal guardians provided written informed consent to the study prior to blood/saliva sampling.

Supporting Information

Additional Supporting Information may be found in the online version of this article at the publisher's website.

References

1 Whitmore SE, Tausk FA. Short anagen syndrome. *J Clin Dermatol* 1999; **2**:30–2.
2 Barraud-Klenovsek MM, Trueb RM. Congenital hypotrichosis due to short anagen. *Br J Dermatol* 2000; **143**:612–17.
3 Segawa Y, Yamasaki K, Otake E *et al.* Short anagen syndrome: a unique short hair syndrome without any characteristic hair morphological abnormality. *J Dermatol* 2020; **47**:e349–51.
4 Starace M, Gurioli C, Carpanese MA *et al.* Short anagen syndrome: a case series and algorithm for diagnosis. *Pediatr Dermatol* 2021; **38**:1157–61.
5 Oberlin KE, Maddy AJ, Martinez-Velasco MA *et al.* Short anagen syndrome: case series and literature review. *Pediatr Dermatol* 2018; **35**:388–91.
6 Doche I, Donati A, Valente NS *et al.* Short anagen syndrome in a girl with curly dark hair and consanguineous parents. *J Am Acad Dermatol* 2012; **67**:e279–80.
7 Antaya RJ, Sideridou E, Olsen EA. Short anagen syndrome. *J Am Acad Dermatol* 2005; **53**:S130–4.
8 Randolph MJ, Gwillim EC, Nguyen B *et al.* The psychologic impact of loose anagen syndrome and short anagen syndrome. *Pediatr Dermatol* 2022; **39**:567–9.
9 Hochfeld LM, Bertolini M, Broadley D *et al.* Evidence for a functional interaction of WNT10A and EBF1 in male-pattern baldness. *PLOS ONE* 2021; **16**:e0256846.
10 Pirastu N, Joshi PK, de Vries PS *et al.* GWAS for male-pattern baldness identifies 71 susceptibility loci explaining 38% of the risk. *Nat Commun* 2017; **8**:1584.
11 Heilmann S, Kiefer AK, Fricker N *et al.* Androgenetic alopecia: identification of four genetic risk loci and evidence for the contribution of WNT signaling to its etiology. *J Invest Dermatol* 2013; **133**:1489–96.
12 Yap CX, Sidorenko J, Wu Y *et al.* Dissection of genetic variation and evidence for pleiotropy in male pattern baldness. *Nat Commun* 2018; **9**:5407.
13 Hagenaars SP, Hill WD, Harris SE *et al.* Genetic prediction of male pattern baldness. *PLOS Genet* 2017; **13**:e1006594.
14 Ü Basmanav FB, Cau L, Tafazzoli A *et al.* Mutations in three genes encoding proteins involved in hair shaft formation cause uncombable hair syndrome. *Am J Hum Genet* 2016; **99**:1292–304.
15 Rentzsch P, Schubach M, Shendure J *et al.* CADD-splice-improving genome-wide variant effect prediction using deep learning-derived splice scores. *Genome Med* 2021; **13**:31.
16 Adzhubei IA, Schmidt S, Peshkin L *et al.* A method and server for predicting damaging missense mutations. *Nat Methods* 2010; **7**:248–9.
17 *R: A Language and Environment for Statistical Computing*. Vienna: R Foundation for Statistical Computing, 2012.

18 Karczewski KJ, Francioli LC, Tiao G *et al.* The mutational constraint spectrum quantified from variation in 141,456 humans. *Nature* 2020; **581**:434–43.
19 Machiela MJ, Chanock SJ. LDlink: a web-based application for exploring population-specific haplotype structure and linking correlated alleles of possible functional variants. *Bioinformatics* 2015; **31**:3555–7.
20 Waterhouse A, Bertoni M, Bienert S *et al.* SWISS-MODEL: homology modelling of protein structures and complexes. *Nucleic Acids Res* 2018; **46**:W296–303.
21 Hirai H, Matoba K, Mihara E *et al.* Crystal structure of a mammalian Wnt-frizzled complex. *Nat Struct Mol Biol* 2019; **26**:372–9.
22 Zhong Q, Zhao Y, Ye F *et al.* Cryo-EM structure of human Wntless in complex with Wnt3a. *Nat Commun* 2021; **12**:4541.
23 Jumper J, Evans R, Pritzel A *et al.* Highly accurate protein structure prediction with AlphaFold. *Nature* 2021; **596**:583–9.
24 Chang CC, Chow CC, Tellier LC *et al.* Second-generation PLINK: rising to the challenge of larger and richer datasets. *Gigascience* 2015; **4**:7.
25 Weissbrod O, Hormozdiari F, Benner C *et al.* Functionally informed fine-mapping and polygenic localization of complex trait heritability. *Nat Genet* 2020; **52**:1355–63.
26 Wang G, Sarkar A, Carbonetto P *et al.* A simple new approach to variable selection in regression, with application to genetic fine mapping. *J R Stat Soc Ser B Stat Methodol* 2020; **82**:1273–300.
27 Zou Y, Carbonetto P, Wang G *et al.* Fine-mapping from summary data with the "Sum of Single Effects" model. *PLOS Genet* 2022; **18**:e1010299.
28 Bohring A, Stamm T, Spaich C *et al.* WNT10A mutations are a frequent cause of a broad spectrum of ectodermal dysplasias with sex-biased manifestation pattern in heterozygotes. *Am J Hum Genet* 2009; **85**:97–105.
29 Doolan BJ, Onoufriadis A, Kantaputra P *et al.* WNT10A, dermatology and dentistry. *Br J Dermatol* 2021; **185**:1105–11.
30 Tsutsumi N, Hwang S, Waghray D *et al.* Structure of the Wnt-Frizzled-LRP6 initiation complex reveals the basis for coreceptor discrimination. *Proc Natl Acad Sci U S A* 2023; **120**:e2218238120.
31 Cluzeau C, Hadj-Rabia S, Jambou M *et al.* Only four genes (EDA1, EDAR, EDARADD, and WNT10A) account for 90% of hypohidrotic/anhidrotic ectodermal dysplasia cases. *Hum Mutat* 2011; **32**:70–2.
32 Martinez-Romero MC, Ballesta-Martinez MJ, Lopez-Gonzalez V *et al.* EDA, EDAR, EDARADD and WNT10A allelic variants in patients with ectodermal derivative impairment in the Spanish population. *Orphanet J Rare Dis* 2019; **14**:281.
33 Song S, Zhao R, He H *et al.* WNT10A variants are associated with non-syndromic tooth agenesis in the general population. *Hum Genet* 2014; **133**:117–24.
34 Plaisancie J, Bailleul-Forestier I, Gaston V *et al.* Mutations in WNT10A are frequently involved in oligodontia associated with minor signs of ectodermal dysplasia. *Am J Med Genet A* 2013; **161A**:671–8.
35 Kantaputra P, Kaewgahya M, Jotikasthira D *et al.* Tricho-odonto-onycho-dermal dysplasia and WNT10A mutations. *Am J Med Genet A* 2014; **164A**:1041–8.
36 Yang J, Wang S-K, Choi M *et al.* Taurodontism, variations in tooth number, and misshapened crowns in Wnt10a null mice and human kindreds. *Mol Genet Genom Med* 2015; **3**:40–58.
37 Heilmann-Heimbach S, Hochfeld LM, Paus R *et al.* Hunting the genes in male-pattern alopecia: how important are they, how close are we and what will they tell us? *Exp Dermatol* 2016; **25**:251–7.
38 Xu M, Horrell J, Snitow M *et al.* WNT10A mutation causes ectodermal dysplasia by impairing progenitor cell proliferation and KLF4-mediated differentiation. *Nat Commun* 2017; **8**:15397.
39 Reddy S, Andl T, Bagasra A *et al.* Characterization of Wnt gene expression in developing and postnatal hair follicles and identification of Wnt5a as a target of Sonic hedgehog in hair follicle morphogenesis. *Mech Dev* 2001; **107**:69–82.
40 Fuchs E. Scratching the surface of skin development. *Nature* 2007; **445**:834–42.
41 Hawkshaw NJ, Hardman JA, Alam M *et al.* Deciphering the molecular morphology of the human hair cycle: Wnt signalling during the telogen-anagen transformation. *Br J Dermatol* 2020; **182**:1184–93.
42 Van Geel M, Gattas M, Kesler Y *et al.* Phenotypic variability associated with WNT10A nonsense mutations. *Br J Dermatol* 2010; **162**:1403–6.
43 Zeng Y, Baugh E, Akyalcin S *et al.* Functional effects of WNT10A rare variants associated with tooth agenesis. *J Dent Res* 2021; **100**:302–9.
44 Cheng Y-P, Chen Y-S, Lin S-J *et al.* Minoxidil improved hair density in an Asian girl with short anagen syndrome: a case report and review of literature. *Int J Dermatol* 2016; **55**:1268–71.
45 Kwack MH, Kang BM, Kim MK *et al.* Minoxidil activates β-catenin pathway in human dermal papilla cells: a possible explanation for its anagen prolongation effect. *J Dermatol Sci* 2011; **62**:154–9.
46 Olsen EA, Dunlap FE, Funicella T *et al.* A randomized clinical trial of 5% topical minoxidil versus 2% topical minoxidil and placebo in the treatment of androgenetic alopecia in men. *J Am Acad Dermatol* 2002; **47**:377–85.

3.2 Publication 2:

Basmanav FB, **Cesarato N**, Kumar S, Borisov O, Kokordelis P, Ralser DJ, Wehner M, Axt D, Xiong X, Thiele H, Dolgin V, Gossmann Y, Fricker N, Dewenter MK, Weller K, Suri M, Reichenbach H, Oji V, Addor MC, Ramirez K, Stewart H, Garcia Bartels N, Weibel L, Wagner N, George S, Kilic A, Tantcheva-Poor I, Stewart A, Dikow N, Blaumeiser B, Medvecz M, Blume-Peytavi U, Farrant P, Grimalt R, Bertok S, Bradley L, Eskin-Schwartz M, Birk OS, Bygum A, Simon M, Krawitz P, Fischer C, Hamm H, Fritz G, Betz RC. Assessment of the Genetic Spectrum of Uncombable Hair Syndrome in a Cohort of 107 Individuals. JAMA Dermatol. 2022; 158: 1245-1253

Research

JAMA Dermatology | Original Investigation

Assessment of the Genetic Spectrum of Uncombable Hair Syndrome in a Cohort of 107 Individuals

F. Buket Basmanav, PhD; Nicole Cesarato, MSc; Sheetal Kumar, MD; Oleg Borisov, PhD; Pavlos Kokordelis, PhD; Damian J. Ralser, MD; Maria Wehner, MSc; Daisy Axt; Xing Xiong, MSc; Holger Thiele, MD; Vadim Dolgin, MD; Yasmina Gossmann, MSc; Nadine Fricker; Malin Katharina Dewenter, MD; Karsten Weller, MD; Mohnish Suri, MD; Herbert Reichenbach, MD; Vinzenz Oji, MD; Marie-Claude Addor, MD; Karla Ramirez, MD; Helen Stewart, MD; Natalie Garcia Bartels, MD; Lisa Weibel, MD; Nicola Wagner, MD; Susannah George, MBBCh; Arzu Kilic, MD; Iliana Tantcheva-Poor, MD; Alison Stewart, MBChB; Nicola Dikow, MD; Bettina Blaumeiser, MD, PhD; Márta Medvecz, MD, PhD; Ulrike Blume-Peytavi, MD, PhD; Paul Farrant, MBBS, BSc; Ramon Grimalt, MD; Sara Bertok, MD; Lisa Bradley, MSc, MB; Marina Eskin-Schwartz, MD, PhD; Ohad Samuel Birk, MD, PhD; Anette Bygum, MD, DMSci; Michel Simon, PhD; Peter Krawitz, MD; Christine Fischer, PhD; Henning Hamm, MD; Günter Fritz, PhD; Regina C. Betz, MD

IMPORTANCE Uncombable hair syndrome (UHS) is a rare hair shaft anomaly that manifests during infancy and is characterized by dry, frizzy, and wiry hair that cannot be combed flat. Only about 100 known cases have been reported so far.

OBJECTIVE To elucidate the genetic spectrum of UHS.

DESIGN, SETTING, AND PARTICIPANTS This cohort study includes 107 unrelated index patients with a suspected diagnosis of UHS and family members who were recruited worldwide from January 2013 to December 2021. Participants of all ages, races, and ethnicities were recruited at referral centers or were enrolled on their own initiative following personal contact with the authors. Genetic analyses were conducted in Germany from January 2014 to December 2021.

MAIN OUTCOMES AND MEASURES Clinical photographs, Sanger or whole-exome sequencing and array-based genotyping of DNA extracted from blood or saliva samples, and 3-dimensional protein modeling. Descriptive statistics, such as frequency counts, were used to describe the distribution of identified pathogenic variants and genotypes.

RESULTS The genetic characteristics of patients with UHS were established in 80 of 107 (74.8%) index patients (82 [76.6%] female) who carried biallelic pathogenic variants in *PADI3*, *TGM3*, or *TCHH* (ie, genes that encode functionally related hair shaft proteins). Molecular genetic findings from 11 of these 80 individuals were previously published. In 76 (71.0%) individuals, the UHS phenotype were associated with pathogenic variants in *PADI3*. The 2 most commonly observed *PADI3* variants account for 73 (48.0%) and 57 (37.5%) of the 152 variant *PADI3* alleles in total, respectively. Two individuals carried pathogenic variants in *TGM3*, and 2 others carried pathogenic variants in *TCHH*. Haplotype analyses suggested a founder effect for the 4 most commonly observed pathogenic variants in the *PADI3* gene.

CONCLUSIONS AND RELEVANCE This cohort study extends and gives an overview of the genetic variant spectrum of UHS based on molecular genetic analyses of the largest worldwide collective of affected individuals, to our knowledge. Formerly, a diagnosis of UHS could only be made by physical examination of the patient and confirmed by microscopical examination of the hair shaft. The discovery of pathogenic variants in *PADI3*, *TCHH*, and *TGM3* may open a new avenue for clinicians and affected individuals by introducing molecular diagnostics for UHS.

JAMA Dermatol. 2022;158(11):1245-1253. doi:10.1001/jamadermatol.2022.2319
Published online August 31, 2022.

Supplemental content

Author Affiliations: Author affiliations are listed at the end of this article.

Corresponding Author: Regina C. Betz, MD, Institute of Human Genetics, University of Bonn, Medical Faculty & University Hospital Bonn, Venusberg-Campus 1, Bldg 13, Bonn 53127, Germany (regina.betz@uni-bonn.de).

© 2022 American Medical Association. All rights reserved.

Uncombable hair syndrome (UHS 1-3; OMIM 191480, 617251, 617252, respectively) is a rare, autosomal recessive disorder characterized by an abnormal hair shaft.[1-3] Dermatologists also refer to UHS as spun glass hair syndrome or pili trianguli et canaliculi. Children with UHS present with dry, frizzy, wiry, and often light-colored, shiny hair that stands out from the scalp and cannot be combed flat. Uncombable hair syndrome usually manifests in infancy or early childhood, frequently improves with age, and in some cases, by adulthood the UHS phenotype becomes barely recognizable. Nevertheless, UHS often leaves a lasting imprint on the childhood years of the affected owing to pejorative responses to their unusual appearance. Although additional clinical features have been reported, such as ectodermal dysplasia, retinitis pigmentosa, juvenile cataract, and polydactyly, UHS typically manifests as an isolated hair anomaly. No medical therapy is yet available.

In 2016, we published, to our knowledge, the first investigation into the molecular genetics of UHS.[1] This investigation included 18 individuals with UHS (13 females and 5 males) and identified biallelic variants in the genes *PADI3* (OMIM 606755), *TCHH* (OMIM 190370), and *TGM3* (OMIM 600238) in 11 individuals. *PADI3*, *TCHH,* and *TGM3* encode proteins whose sequential interactions play a role in the formation of the hair shaft.[4,5] *PADI3* is responsible for the deimination of the positively charged L-arginine residues of proteins into neutral citrulline residues in the presence of calcium ions.[5] One of the main substrates of *PADI3* is the structural hair shaft protein trichohyalin (TCHH). Deimination by *PADI3* reduces the overall charge of TCHH and thus enables its subsequent interaction with the intermediate keratin filaments. The citrullinated-TCHH and keratin filaments are then cross-linked by the TGM3 enzyme, a process that is necessary for the stabilization and hardening of the hair shaft.[4-7] Disturbance of this cascade leads to a deficiency in the shaping and mechanical strengthening of the hair shaft, thus resulting in the UHS phenotype.[1]

Prior to our 2016 study,[1] the assignment of a clinical diagnosis of UHS was mainly based on signs detected during a clinical examination, with confirmation via shrinking-tube technique light microscopy or scanning electron microscopy of hair shaft cross sections.[8] In at least 50% of examined hair samples, scanning electron microscopy reveals longitudinal grooves along the entire length of the hair shaft and a triangular or heart-shaped outline in the cross-section, as opposed to the normal circular shape.[9] As a direct consequence of our study,[1] we now base the assignment or confirmation of a clinical diagnosis of UHS on molecular genetic diagnostics.

At the time of our 2016 report,[1] around 100 cases of UHS had been reported. Subsequent to our report, we were contacted by a large number of clinicians and members of the public from across the world with information on further possible UHS cases. Several of the individuals from the general public reported having had a history of UHS symptoms during childhood, without the assignment of a clinical diagnosis. As a result of these contacts, EDTA blood samples, saliva, or DNA were sent to our laboratory from 89 unrelated index patients. For 51 of these patients, samples were also received from affected and/or unaffected family members. We obtained DNA to screen an affected sibling or an affected parent in 7 and 2 families, respectively. Herein, we report the results of the molecular genetic analyses.

Key Points

Question What is the genetic spectrum of uncombable hair syndrome (UHS)?

Findings This cohort study of 107 index patients describes pathogenic variants in 80 individuals with a suspected diagnosis of UHS in the genes *PADI3*, *TCHH*, and *TGM3*. Of these individuals, 76 carried 12 different pathogenic variants in *PADI3*, 2 carried 3 pathogenic variants in *TCHH*, and 2 carried 3 pathogenic variants in *TGM3*; a haplotype analysis suggested a founder effect for the 4 most common pathogenic *PADI3* variants.

Meaning This study expands the genotypic spectrum of UHS and establishes that 2 pathogenic missense variants in *PADI3* account for the majority of the UHS cases.

Methods

Participants

All study procedures were performed in accordance with the principles of the Declaration of Helsinki. Ethical approval was obtained from the ethics committee of the Medical Faculty of the University of Bonn, and all participants, or legal guardians in the case of minors, provided written informed consent prior to blood sampling. The countries of origin of the respective individuals who were genetically elucidated are presented in relation to the identified pathogenic variants to provide an overview of the diversity of the UHS-related genetic variation spectrum worldwide. Note that this information is not equivalent to race or ethnicity. This study followed the Strengthening the Reporting of Observational Studies in Epidemiology (STROBE) reporting guideline.

Genetic Analyses

Sanger sequencing was performed using the BigDye Terminator v.1.1 Cycle Sequencing Kit (Applied Biosystems) and an ABI 3100 genetic analyzer (Applied Biosystems). Exome sequencing was performed at the Cologne Center for Genomics in Cologne, Germany. Data generation and filtering procedures are described in detail in the eMethods in the Supplement. Haplotype analysis was performed for the 4 most commonly observed pathogenic variants in *PADI3* using single-nucleotide polymorphism (SNP) chip data as described in detail in the eMethods in the Supplement.

Results

In addition to the 18 individuals reported in our 2016 study,[1] genetic screening of an additional 89 unrelated individuals with suspected UHS (69 females and 20 males) led to the identification of pathogenic variants in 69 of them. The affected individuals presented with the typical dry, frizzy, and shiny hair

© 2022 American Medical Association. All rights reserved.

Figure 1. Clinical Manifestation of Uncombable Hair Syndrome (UHS)

The typical manifestation of UHS with shiny, frizzy, and dry hair can be observed in 8 individuals carrying biallelic pathogenic variants in the *PADI3* gene. See eFigure 1 in the Supplement for more individuals (n = 22) with their respective genotypes.

that was difficult to be combed flat (**Figure 1** and eFigure 1 in the Supplement). Sixty-seven of these individuals harbored recurrent and/or novel pathogenic variants in *PADI3* in either a homozygous or a compound heterozygous state, and 2 individuals carried previously unreported compound heterozygous pathogenic variants in either *TGM3* or *TCHH*. From the newly elucidated 67 individuals with pathogenic *PADI3* variants, 56 carried 1 or 2 of the 4 variants reported in our 2016 study.[1] In the remaining 11 individuals, the following 8 previously unreported pathogenic *PADI3* (NM_016233.2) variants were identified: c.60_66delinsTGCTTGG (p.Gly22Trp); c.505C>T (p.Gln169*); c.556C>T (p.Arg186Trp); c.652G>A (p.Gly218Ser); c.1114A>G (p.Arg372Gly); c.1115G>T (p.Arg372Met); c. 1183del (p.Glu395Asnfs*7); and c.1868C>T (p.Pro623Leu) (**Figure 2**). This expands the UHS-associated variant spectrum of *PADI3* to a total of 12 pathogenic variants identified in individuals from 20 countries (eTable 1 in the Supplement). Of these, 9 lead to single amino acid substitutions, 2 are nonsense variants, and 1 is a frameshift variant leading to a premature stop codon.

To examine the possible consequences of the newly discovered *PADI3* variants on 3-dimensional protein structure and function, protein modeling was performed (**Figure 3** and eFigure 2 in the Supplement). Interestingly, 2 of the newly discovered missense variants (p.Arg372Gly and p.Arg372Met) affect the same amino acid residue Arg372, which is involved in substrate binding via the formation of hydrogen bonds with the substrate arginine (Figure 3B). Modeling revealed that substitution of this residue by glycine or methionine results in the loss of these hydrogen bonds (Figure 3B). This is presumably associated with weaker substrate binding and lower enzyme activity.

The modeling also demonstrated that 2 other missense variants have probable consequences on the stability of *PADI3*. More specifically, substitution of arginine 186 to tryptophan results in the loss of stabilizing hydrogen bonds (Figure 3C). Substitution of glycine 22 to tryptophan results in the insertion of a bulky residue in a β-turn (Figure 3D). β-Turn loops require a small residue allowing for flexibility. Thus, in all β-turn loops, glycine is the most frequent residue in this position. The replacement of glycine by any other amino acid residue will destabilize the protein.[10] The most common previously reported pathogenic missense variants in *PADI3* were also remodeled and showed that the residues Leu112, Ala294, and

© 2022 American Medical Association. All rights reserved.

Figure 2. Additional Pathogenic Variants in *PADI3*

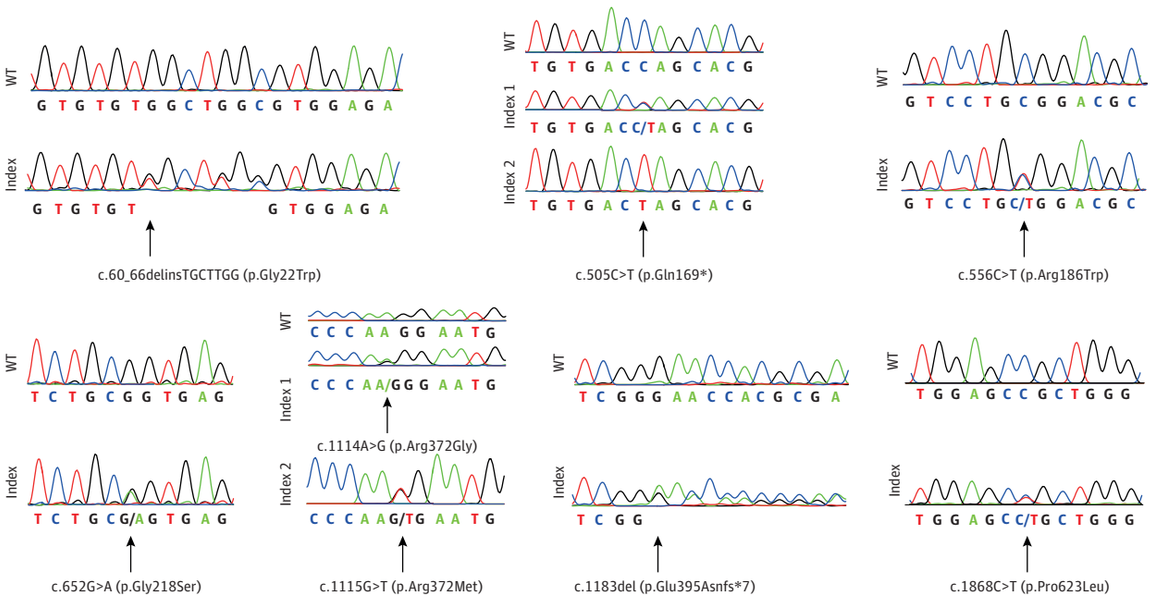

Electropherograms showing the newly discovered pathogenic variants c.60_66delinsTGCTTGG (p.Gly22Trp), c.505C>T (p.Gln169*) in heterozygosity and homozygous state, c.556C>T (p.Arg186Trp), c.652G>A (p.Gly218Ser), c.1114A>G (p.Arg372Gly), c.1115G>T (p.Arg372Met), c.1183del (p.Glu395Asnfs*7), and c.1868C>T (p.Pro623Leu) in comparison with the respective wild-type (WT) sequences. The 2 variants c.1114A>G (p.Arg372Gly) and c.1115G>T (p.Arg372Met) are located adjacently and therefore depicted below the same wild-type sequence. Of note, variant c.60_66delinsTGCTTGG (p.Gly22Trp) may also represent a rare haplotype composed of 3 single nucleotide variants, namely rs1360902614, rs1221559173, and rs1344213588, which have been observed in the same single individual (minor allele frequency = 6.5×10^{-6}) in gnomAD (Genome Aggregation Database).

Pro605 are located in the hydrophobic core of the enzyme (eFigure 3 in the Supplement). The substitution of these residues by amino acids with larger side chains causes sterical clashes (eFigure 3 in the Supplement) in the hydrophobic core of the protein, and thus most likely destabilizes *PADI3*.

For *TCHH* (NM_007113.3), our 2016 study[1] identified 1 individual with the pathogenic homozygous stop variant c.991C>T (p.Gln331*). In the expanded cohort, there was 1 individual identified with compound heterozygosity for 2 novel *TCHH* frameshift variants, each of which leads to a premature stop codon: c.2435del (p.Pro812Argfs*67) and c.4245del (p.Lys1415Asnfs*9) (**Figure 4**A).

Notably, 2 individuals in the present cohort carried only 1 heterozygous loss-of-function variant in *TCHH*, c.991C>T (p.Gln331*) and the novel frameshift variant c.4005_4008del (p.Asp1335Glufs*88), respectively. No second pathogenic variant in the coding sequence was detected for either individual. In these 2 individuals, a plausible hypothesis is the existence of a structural variant on the other allele, the detection of which may be challenged by short-read exomes or Sanger sequencing. Until this is investigated further, the genetic cause of these 2 cases remains unclear.

In our 2016 study,[1] 1 individual was identified with the pathogenic homozygous stop variant c.1351C>T (p.Gln451*) in *TGM3*. In the expanded cohort, 1 individual was identified with 2 rare pathogenic missense variants in *TGM3* (NM_003245.3) in a compound heterozygous state: c.1966C>T (p.Arg656Trp) (rs151074346 with a minor allele frequency in the Genome Aggregation Database [gnomAD] = 5.00×10^{-4}) and c.1993C>T (p.Arg665Trp) (rs150949349 with a minor allele frequency in gnomAD = 3.16×10^{-3}) (Figure 4B). Protein modeling suggests that the Arg665Trp variation destabilizes the contact of the C-terminal barrel 2 domain with the core domain. Arg665 forms 2 hydrogen bonds with the side chain of Asp156 and the backbone carbonyl of Lys24. Both hydrogen bonds are lost by mutation to Trp (Figure 4C). The Arg656Trp substitution will most likely not affect protein stability but will decrease the surface charge of the barrel 2 domain.

The total present cohort included 107 unrelated index patients with UHS. For 80 (74.8%) of these patients, the genetic associations have been established, while for 27 (25.2%), the pathogenic variants/associated genes remain unknown (**Figure 5**A). Briefly, in 76 (71.0%) individuals, the UHS phenotype was associated with biallelic variants in *PADI3*, while *TGM3* and *TCHH* together (2 individuals each) were associated with only 3.8% of the UHS cases.

The most recurrent pathogenic *PADI3* variants were c.881C>T (p.Ala294Val) and c.335T>A (p.Leu112His) (73 [48.0%] and 57 [37.5%] of 152 pathogenic *PADI3* alleles identified in total, respectively; Figure 5B). Of the 76 individuals with *PADI3* pathogenic variants, 75 carried either 1 or both of these variants. On the genotype level, 29 of 76 (38.2%) individuals, whose UHS was associated with *PADI3*, had a combination of these 2 pathogenic variants; 18 (23.7%) carried c.881C>T (p.Ala294Val)

© 2022 American Medical Association. All rights reserved.

Figure 3. Three-Dimensional Protein Modeling of Newly Discovered *PADI3* Variants

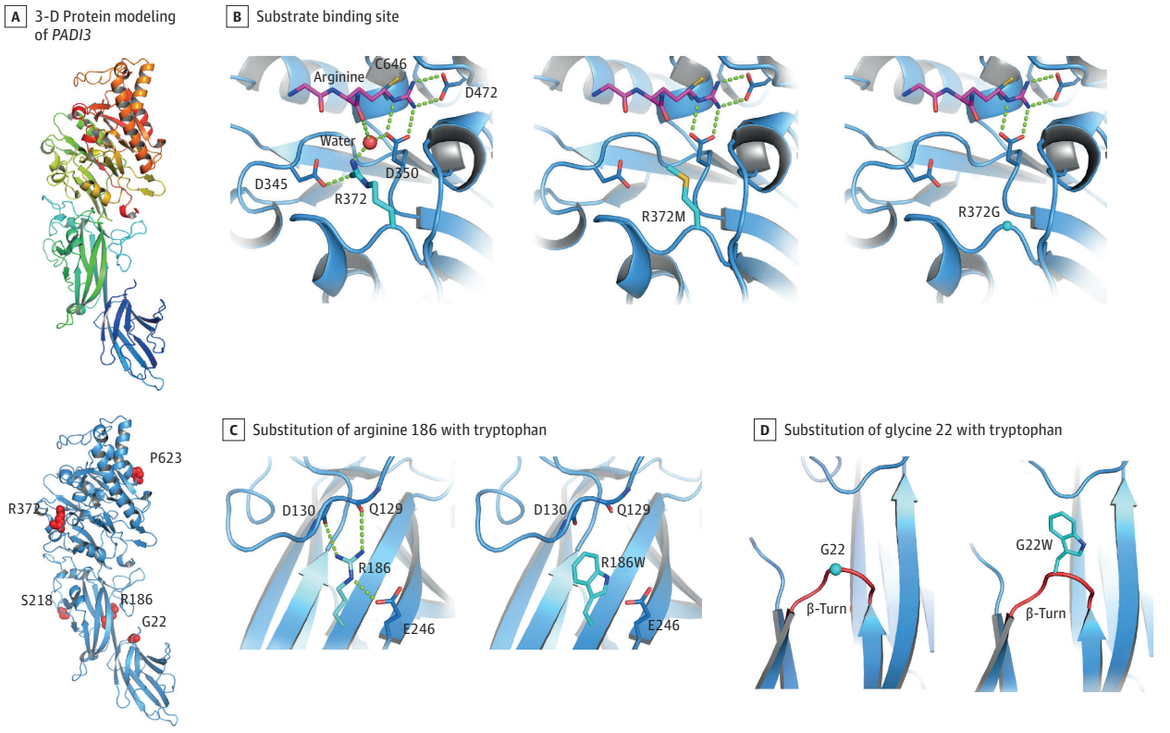

An overview of the entire 3-dimensional model of the wild-type *PADI3* gene (A, upper panel) and the locations of the newly identified missense substitutions (A, bottom panel). Arginine 372 is located at the substrate binding site of *PADI3* and is involved in the binding of L-arginine residues of target proteins via formation of hydrogen bonds (B, left); its substitution by a methionine (B, middle) or glycine (B, right) is expected to lead to the loss of these hydrogen bonds, thus a weaker substrate binding and lower enzyme activity. Substitution of arginine 186 in the wild-type *PADI3* gene (C, left) with a tryptophan (C, right), as well as substitution of glycine 22 (D, left) with a tryptophan (D, right), are expected to destabilize *PADI3* owing to loss of stabilizing hydrogen bonds (C) and insertion of a bulky residue in a β-turn loop reducing the flexibility at this site (D).

in a homozygous state, 8 (10.5%) carried c.335T>A (p.Leu112His) in a homozygous state, and 20 (26.3%) carried either one of these variants in combination with another pathogenic variant (Figure 5C). The third most commonly observed recurrent pathogenic variant, c.1813C>A (p.Pro605Thr) (9 of 152 [5.9%] pathogenic *PADI3* alleles identified in total; Figure 5B), was observed in a heterozygous state in 9 of the 76 (11.8%) individuals with a *PADI3* variant (Figure 5C). The newly identified stop variant c.505C>T (p.Gln169*) was the fourth most common pathogenic variant (4 of 152 [2.6%] variant alleles; Figure 5B). This was carried by 3 individuals, with 1 showing a homozygous state (Figure 5C). One missense variant, c.652G>A (p.Gly218Ser), was carried by 2 individuals, and the remaining pathogenic variants were all single heterozygous observations (Figure 5C).

Interestingly, the cohort included 3 families, which include affected parent-child duos who appear to have an autosomal dominant mode of inheritance. For 2 of these families, DNA was also received from the affected parent, and it was confirmed that they each carried 2 pathogenic *PADI3* variants (eFigure 4 in the Supplement). More specifically, in 1 family both the affected mother and son carried p.Leu112His and p.Arg294Val (eFigure 4A in the Supplement). In the other family, the affected mother and daughter carried p.Leu112His in homozygosity. For the latter case, DNA was also available from the unaffected father, and he was found to be a heterozygous carrier of p.Leu112His (eFigure 4B in the Supplement). These results revealed that also in these families, a recessive inheritance was present rather than dominant.

A haplotype analysis for the 4 most common pathogenic *PADI3* variants was performed using genotype data of 40 individuals from 34 families to investigate whether these variants derive from a single mutational event (common ancestor) or have arisen independently multiple times. Shared haplotype blocks of variable sizes were detected in all of the investigated individuals for each of the 4 pathogenic variants with common or individual haplotype break points (Figure 5D and eTables 2-5 and eFigure 5 in the Supplement). The minimally shared haplotype block across all haplotypes carrying c.335T>A (p.Leu112His) was 47.744 base pairs (bp) long and tagged by 19 SNPs, 11 of which were intergenic (Figure 5D). The individual shortest and longest common haplotype blocks detected were 64.919 and 1.606.067 bp long, respectively, and 2 families from Germany shared the latter with the same haplotype break points

© 2022 American Medical Association. All rights reserved.

Figure 4. Newly Discovered Pathogenic Variants in *TCHH* and *TGM3*

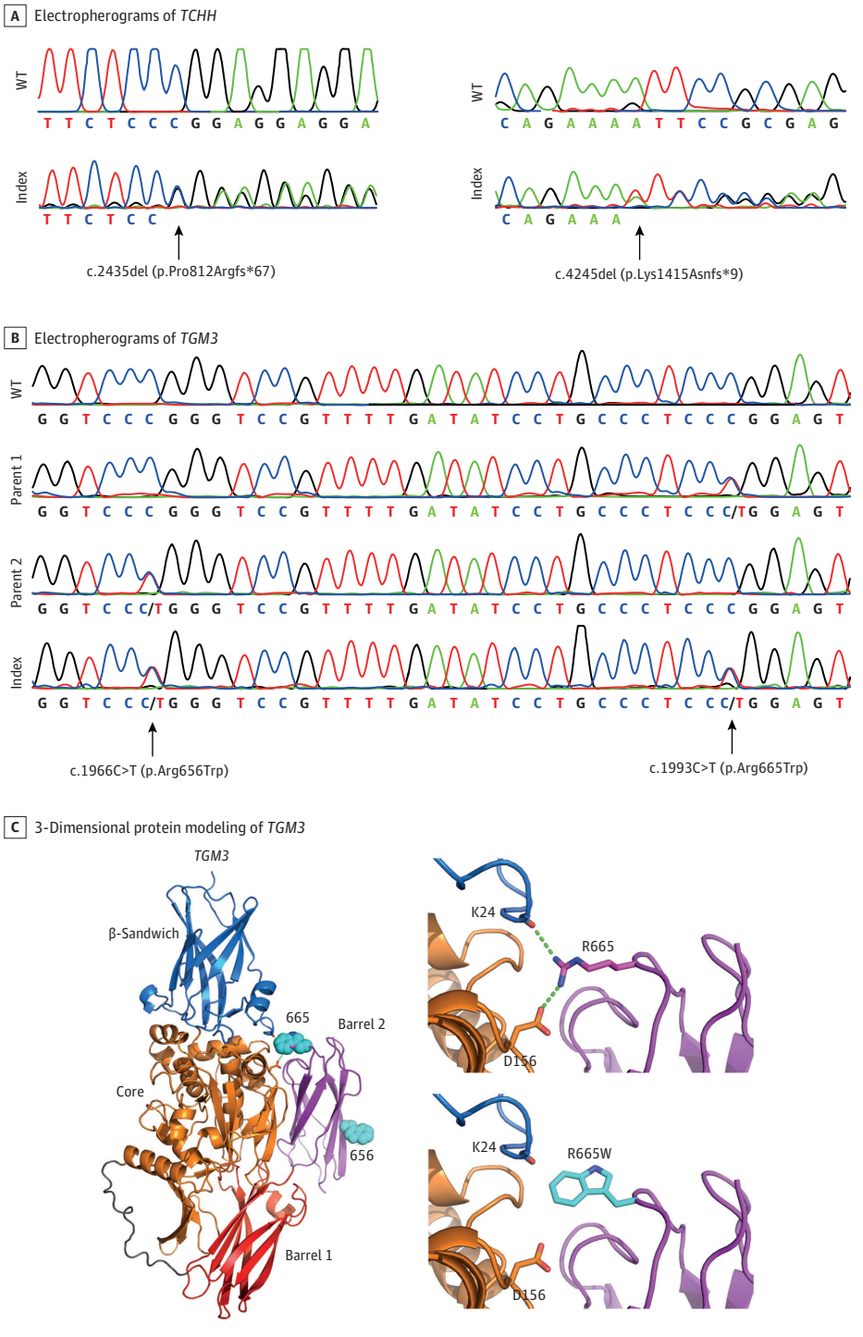

Electropherograms showing the newly discovered pathogenic frameshift variants c.2435del (p.Pro812Argfs*67) and c.4245del (p.Lys1415Asnfs*9) in *TCHH* (A) and the compound heterozygous pathogenic missense variants c.1966C>T (p.Arg656Trp) and c.1993C>T (p.Arg665Trp) in *TGM3* (B) in comparison with the respective wild-type (WT) sequences. Protein modeling suggests that mutation p.Arg665Trp leads to the loss of 2 hydrogen bonds destabilizing the contact of barrel 2 domain to the core domain (C). Domain organization of *TGM3* and location of residues 656 and 655 is indicated (C, left). Arg655 forms hydrogen bonds to the side chain of Asp156 and the backbone carbonyl of Lys24 (C, right upper panel). The mutation of Arg655 to Trp abolishes these hydrogen bonds (C, right lower panel).

(eTable 3 and eFigure 5 in the Supplement). Haplotype sharing between at least 2 individuals was observed up to 466 and 169 SNPs upstream and downstream of the pathogenic variant, respectively. Notably, several common haplotype breakpoints were observed across multiple individuals both upstream and downstream of the site of the pathogenic variation (eTable 3 and eFigure 5 in the Supplement).

The minimally shared haplotype block across all haplotypes carrying c.881C>T (p.Ala294Val) was 34.820 bp long and tagged by 11 SNPs, 10 of which were intragenic (Figure 5D). Notably, a larger block of 99.064 bp long was shared between 31 of the 34 (91.1%) investigated haplotypes carrying this variant. The individual shortest and longest common haplotype blocks detected were 51.669 and 1.674.521 bp long, respectively.

© 2022 American Medical Association. All rights reserved.

Figure 5. Genetic Spectrum of UHS and Common Haplotypes Surrounding the Most Common *PADI3* Pathogenic Variants

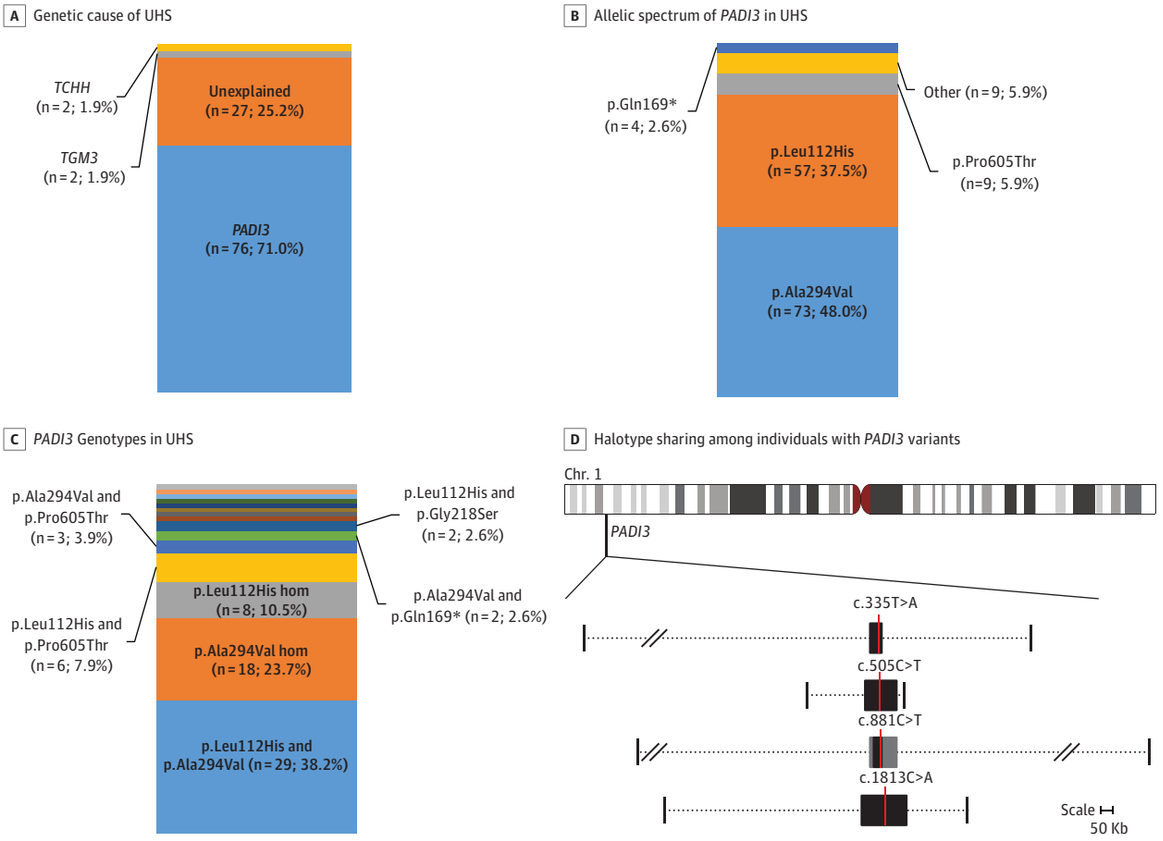

A, Stacked percentage bar plots depict the respective proportion of affected index cases that could be explained by pathogenic variants in either 1 of the 3 known uncombable hair syndrome (UHS)-associated genes and those not yet genetically elucidated within the total cohort. B, Individual pathogenic variants within all mutated *PADI3* alleles (other includes p.Gly22Trp [n = 1], p.Arg186Trp [n = 1], p.Gly218Ser [n = 2], p.Arg372Gly [n = 1], p.Arg372Met [n = 1], p.Glu395Asnfs*7 [n = 1], p.Lys578* [n = 1], and p.Pro623Leu [n = 1]). C, Pathogenic genotypes within all *PADI3*-associated UHS cases: p.Gln169* homozygous; p.Leu112His and p.Glu395Asnfs*7; p.Leu112His and Arg186Trp; p.Leu112His and p.Arg372Met; p.Leu112His and p.Gly22Trp; p.Ala294Val and p.Arg372Gly; p.Ala294Val and p.Pro623Leu; and p.Ala294Val and p.Lys578* were singleton observations represented with different color codes without text, and each constitutes approximately 1% of the bar plot. D, The minimally shared regions across all haplotypes carrying a pathogenic variant are denoted with black boxes, and the location of the respective variations are depicted with a red line. The gray boxes surrounding c.881C>T denote a common haplotype shared over 90% of all analyzed haplotypes. The variable extent of haplotype sharing across all analyzed samples is denoted by the dotted lines, whereby the vertical lines on either end of the dotted lines mark the furthest extent of haplotype sharing between at least 2 samples upstream and downstream of the respective pathogenic variants. Slash marks show omitted whole sizes owing to space restraints. See eFigure 5 and eTables 2 through 5 in the Supplement for a depiction of haplotype sharing on individual level.

Haplotype sharing between at least 2 individuals was observed up to 378 and 306 SNPs upstream and downstream of the pathogenic variant, respectively, and similar to c.335T>A (p.Leu112His); common breakpoints were observed on either side of the pathogenic variant (eTable 4 and eFigure 5 in the Supplement).

For the third most common pathogenic variant c.1813C>A (p.Pro605Thr), 4 haplotypes were analyzed (eTable 5 in the Supplement). The minimally shared haplotype block across them was 162.538 bp long (Figure 5D), exceeding *PADI3* and extending over the neighboring genes *PADI1* and *PADI4*. Haplotype sharing between at least 2 individuals was observed up to 230 and 88 SNPs upstream and downstream of the pathogenic variant, respectively. The minimally shared haplotype block across all haplotypes carrying c.505C>T (p.Gln169*) was 116.238 bp long (Figure 5D) and also extended over the neighboring genes *PADI1* and *PADI4*. Haplotype sharing between at least 2 individuals was observed up to 144 and 34 SNPs upstream and downstream of the pathogenic variant, respectively (eTable 2 in the Supplement). Altogether, these results support the founder mutation hypothesis for each of the 4 analyzed pathogenic variants.

Discussion

Taken together, the present results show that in the majority of the present cohort, UHS was associated with pathogenic

© 2022 American Medical Association. All rights reserved.

variants in the gene *PADI3*, including 2 recurrent variants that were detected in around 99% of all *PADI3* variant carriers. The present study led to discovery of 8 novel pathogenic variants in *PADI3*. Of these, 6 were single observations and 2 were observed in 3 and 2 individuals, respectively. Therefore, we anticipate that other very rare pathogenic variants in *PADI3* exist and that these are likely to be discovered in the future.

Remarkably, in 3 of the newly referred families, the examination of exome sequencing data revealed pathogenic variants in either *LIPH* (2 families) or *LPAR6* (1 family) genes (ie, genes underlying hypotrichosis simplex with woolly hair). This suggests that the woolly hair phenotype (with or without hypotrichosis) may be mistaken for UHS by clinicians or affected individuals and, therefore, we suggest that woolly hair should be considered in the differential diagnosis of UHS.

In the present cohort, all of the individuals with pathogenic variants in *PADI3*, *TGM3*, or *TCHH* showed an autosomal recessive mode of inheritance. In the literature prior to the genetic elucidation of UHS, some pedigrees were reported who appeared to have an autosomal dominant inheritance with a respective affected parent. In this cohort, we performed genetic screening in 2 such families with an apparent autosomal dominant mode of inheritance. The results indeed revealed a pseudodominance because the affected parents also happened to be carriers of biallelic *PADI3* variants even though the child had inherited the phenotype in an autosomal recessive fashion. In fact, this was not surprising because the allele frequency of some of the pathogenic *PADI3* variants is not very low in the population (eTable 1 in the Supplement). Therefore, we suggest that at least some of those pedigrees from the literature with a presumed autosomal dominant mode of inheritance may in fact also have an autosomal recessive inheritance of pathogenic *PADI3* variants similar to the 2 families reported herein. However, given that the genetic associations of around one-fourth of the cohort remains unclear, another plausible hypothesis is that pathogenic variants in other genes may also be associated with UHS and that some of these genes may have an autosomal dominant pattern of inheritance. Nonetheless, based on the exome data of the genetically unclarified cases, we can assume that the UHS phenotype is unlikely to be related to a fourth major gene that is recurrently affected by pathogenic coding variants. We therefore speculate that a large heterogeneity may exist with several other UHS-associated genes, each of which may explain the phenotype in only a single or very few families, as is the case for *TCHH* and *TGM3*.

Limitations

It cannot be excluded that some of the unexplained cases may be related to variants that affect the splicing or expression of known UHS-associated genes and have remained undetected by the sequencing approaches used here. In fact, it is well known that large structural variants such as deletions/duplications and complex rearrangements are difficult to detect via short-read sequencing approaches. Similarly, deep introns and regulatory regions such as promoters are mostly not covered by whole-exome or Sanger sequencing. Accordingly, we plan in the near future to use a targeted long-read sequencing approach for screening of the entire coding and noncoding regions in and around the known UHS-associated genes in all of the unexplained cases to address this concern.

Conclusions

This cohort study expands the pathogenic variant spectrum of UHS and found that *PADI3* was most commonly associated with this rare hair phenotype. The present results also suggest that the 4 most commonly observed pathogenic *PADI3* variants are far more likely to have descended from a respective common ancestor rather than having had occurred independently multiple times.

ARTICLE INFORMATION

Accepted for Publication: April 29, 2022.

Published Online: August 31, 2022. doi:10.1001/jamadermatol.2022.2319

Author Affiliations: Institute of Human Genetics, Medical Faculty & University Hospital Bonn, University of Bonn, Bonn, Germany (Basmanav, Cesarato, Kumar, Kokordelis, Ralser, Wehner, Axt, Xiong, Gossmann, Fricker, Betz); Institute for Genomic Statistics and Bioinformatics, Medical Faculty & University Hospital Bonn, University of Bonn, Bonn, Germany (Borisov, Krawitz); Cologne Center for Genomics, University of Cologne, Cologne, Germany (Thiele); Genetics Institute at Soroka University Medical Center, Beer-Sheva, Israel (Dolgin, Eskin-Schwartz, Birk); Morris Kahn Laboratory of Human Genetics, National Center for Rare Diseases at the Faculty of Health Sciences, Ben-Gurion University of the Negev, Beer-Sheva, Israel (Dolgin); National Institute for Biotechnology in the Negev, Ben-Gurion University of the Negev, Beer-Sheva, Israel (Dolgin); Institute of Human Genetics, University Medical Center of the Johannes Gutenberg University Mainz, Mainz, Germany (Dewenter); Department of Dermatology, Venereology and Allergology, Charité-Universitätsmedizin Berlin, Berlin, Germany (Weller, Garcia Bartels, Blume-Peytavi); Nottingham Clinical Genetics Service, Nottingham University Hospitals NHS Trust, City Hospital Campus, Nottingham, England, United Kingdom (Suri); MVZ Mitteldeutscher Praxisverbund Humangenetik, Praxis Leipzig, Leipzig, Germany (Reichenbach); Department of Dermatology, University of Münster, Münster, Germany (Oji); Department of Woman-Mother-Child, University Hospital Center CHUV CH 1011, Lausanne, Switzerland (Addor); Neurología Pediátrica, Division de Pediatría, Escuela de Medicina, Pontificia Universidad Católica de Chile, Santiago, Chile (Ramirez); Oxford Centre for Genomic Medicine, Oxford University Hospitals NHS Foundation Trust, Oxford, England, United Kingdom (H. Stewart); Pediatric Dermatology Department, University Children's Hospital Zurich, University Hospital Zurich, Zurich, Switzerland (Weibel); Dermatology Department, University Hospital Zurich, Zurich, Switzerland (Weibel); Department of Dermatology, Universitätsklinikum Erlangen, Friedrich-Alexander-University Erlangen-Nürnberg (FAU), Erlangen, Germany (Wagner); Dermatology Department, Brighton General Hospital, University Hospitals Sussex NHS Foundation Trust, Brighton, England, United Kingdom (George, Farrant); Department of Dermatology, Faculty of Medicine, Balıkesir University, Balıkesir, Turkey (Kilic); Department of Dermatology and Venereology, University Hospital of Cologne, Cologne, Germany (Tantcheva-Poor); Sheffield Clinical Genetics Service, Sheffield Children's Hospital, South Yorkshire, England, United Kingdom (A. Stewart); Institute of Human Genetics, Heidelberg University, Heidelberg, Germany (Dikow, Fischer); Department of Medical Genetics, University of Antwerp, Antwerp, Belgium (Blaumeiser); Department of Dermatology, Venereology, and Dermatooncology, Semmelweis University, Budapest, Hungary (Medvecz); Universitat Internacional de Catalunya, Barcelona, Spain (Grimalt); Department of Pediatric Endocrinology, Diabetes and Metabolic Diseases, University Children's Hospital, University Medical Centre, Ljubljana, Slovenia (Bertok); Department of Clinical Genetics, Children's Health Ireland (CHI) at Crumlin, Dublin, Ireland (Bradley); Department of Clinical Genetics, Odense University Hospital, Odense, Denmark (Bygum); Clinical Institute, University of Southern Denmark, Odense, Denmark

© 2022 American Medical Association. All rights reserved.

(Bygum); Toulouse Institute for Infectious and Inflammatory diseases, Toulouse University, Toulouse, France (Simon); CNRS, Inserm, Paul Sabatier Toulouse III University, Toulouse, France (Simon); Department of Dermatology, Venereology, and Allergology, University Hospital Würzburg, Würzburg, Germany (Hamm); Department of Cellular Microbiology, University of Hohenheim, Stuttgart, Germany (Fritz).

Author Contributions: Dr Basmanav and Prof Betz had full access to all the data in the study and take responsibility for the integrity of the data and the accuracy of the data analysis. Ms Cesarato and Dr Kumar contributed equally to this work.
Concept and design: Basmanav, Betz.
Acquisition, analysis, or interpretation of data: All authors.
Drafting of the manuscript: Basmanav, Fritz, Betz.
Critical revision of the manuscript for important intellectual content: Basmanav, Cesarato, Kumar, Borisov, Kokordelis, Ralser, Wehner, Axt, Xiong, Thiele, Dolgin, Gossmann, Fricker, Dewenter, Weller, Suri, Reichenbach, Oji, Addor, Ramirez, H. Stewart, Garcia Bartels, Weibel, Wagner, George, Kilic, Tantcheva-Poor, A. Stewart, Dikow, Blaumeiser, Medvecz, Blume-Peytavi, Farrant, Grimalt, Bertok, Bradley, Eskin-Schwartz, Birk, Bygum, Simon, Krawitz, Fischer, Hamm, Betz.
Statistical analysis: Borisov, Krawitz, Fischer.
Obtained funding: Betz.
Administrative, technical, or material support: Cesarato, Kumar, Kokordelis, Ralser, Wehner, Axt, Xiong, Thiele, Dolgin, Gossmann, Fricker, Dewenter, Reichenbach, Oji, Addor, Ramirez, H. Stewart, Garcia Bartels, Weibel, Wagner, George, Kilic, Tantcheva-Poor, A. Stewart, Dikow, Blaumeiser, Medvecz, Blume-Peytavi, Grimalt, Bradley, Birk, Bygum, Simon, Hamm, Betz.
Supervision: Basmanav, Kokordelis, Betz.

Conflict of Interest Disclosures: Dr George reported personal fees from Pfizer and nonfinancial support from Sanofi outside the submitted work. No other disclosures were reported.

Funding/Support: This work was supported by a grant from the German-Israeli Foundation for Scientific Research and Development (I-1443-422.13/2017) to Prof Betz, the Deutsche Forschungsgemeinschaft under the auspices of the Germany Excellence Strategy (EXC2151-390873048) to Prof Betz, and grants from the Morris Kahn Foundation to Dr Dolgin.

Role of the Funder/Sponsor: The funders had no role in the design and conduct of the study; collection, management, analysis, and interpretation of the data; preparation, review, or approval of the manuscript; and decision to submit the manuscript for publication.

Additional Contributions: We thank all of the individuals and their families for their support and participation in this study, as well as their permission to publish this information.

Additional Information: Data sets related to this article are available on reasonable request to the first and corresponding authors.

REFERENCES

1. Ü Basmanav FB, Cau L, Tafazzoli A, et al. Mutations in three genes encoding proteins involved in hair shaft formation cause uncombable hair syndrome. *Am J Hum Genet*. 2016;99(6):1292-1304. doi:10.1016/j.ajhg.2016.10.004

2. Calderon P, Otberg N, Shapiro J. Uncombable hair syndrome. *J Am Acad Dermatol*. 2009;61(3):512-515. doi:10.1016/j.jaad.2009.01.006

3. Navarini AA, Kaufmann F, Kaech A, Trüeb RM, Weibel L. Picture of the month: uncombable hair (pili trianguli et canaliculi). *Arch Pediatr Adolesc Med*. 2010;164(12):1165-1166. doi:10.1001/archpediatrics.2010.228-a

4. Tarcsa E, Marekov LN, Andreoli J, et al. The fate of trichohyalin: sequential post-translational modifications by peptidyl-arginine deiminase and transglutaminases. *J Biol Chem*. 1997;272(44):27893-27901. doi:10.1074/jbc.272.44.27893

5. Méchin MC, Takahara H, Simon M. Deimination and peptidylarginine deiminases in skin physiology and diseases. *Int J Mol Sci*. 2020;21(2):566. doi:10.3390/ijms21020566

6. Steinert PM, Parry DA, Marekov LN. Trichohyalin mechanically strengthens the hair follicle: multiple cross-bridging roles in the inner root sheath. *J Biol Chem*. 2003;278(42):41409-41419. doi:10.1074/jbc.M302037200

7. Westgate GE, Botchkareva NV, Tobin DJ. The biology of hair diversity. *Int J Cosmet Sci*. 2013;35(4):329-336. doi:10.1111/ics.12041

8. Kiliç A, Oğuz D, Can A, Akil H, Gürbüz Köz O. A case of uncombable hair syndrome: light microscopy, trichoscopy and scanning electron microscopy. *Acta Dermatovenerol Croat*. 2013;21(3):209-211.

9. Hicks J, Metry DW, Barrish J, Levy M. Uncombable hair (cheveux incoiffables, pili trianguli et canaliculi) syndrome: brief review and role of scanning electron microscopy in diagnosis. *Ultrastruct Pathol*. 2001;25(2):99-103. doi:10.1080/01913120117514

10. Shapovalov M, Vucetic S, Dunbrack RL Jr. A new clustering and nomenclature for beta turns derived from high-resolution protein structures. *PLoS Comput Biol*. 2019;15(3):e1006844. doi:10.1371/journal.pcbi.1006844

© 2022 American Medical Association. All rights reserved.

3.3 Publication 3:

Cesarato N, Wehner M, Ghughunishvili M, Schmidt A, Axt D, Thiele H, Lentze MJ, Has C, Geyer M, Basmanav FB, Betz RC. Four hypotrichosis families with mutations in the gene LSS presenting with and without neurodevelopmental phenotypes. Am J Med Genet A. 2021; 185: 3900-3904

Check for updates

Received: 26 February 2021 | Revised: 12 May 2021 | Accepted: 3 July 2021

DOI: 10.1002/ajmg.a.62438

RESEARCH LETTER

AMERICAN JOURNAL OF medical genetics PART A WILEY

Four hypotrichosis families with mutations in the gene *LSS* presenting with and without neurodevelopmental phenotypes

Nicole Cesarato[1] | Maria Wehner[1] | Mariam Ghughunishvili[2] | Axel Schmidt[1] | Daisy Axt[1] | Holger Thiele[3] | Michael J. Lentze[4] | Cristina Has[5] | Matthias Geyer[6] | Fitnat Buket Basmanav[1] | Regina C. Betz[1]

[1]Institute of Human Genetics, University of Bonn, School of Medicine & University Hospital Bonn, Bonn, Germany

[2]Givi Zhvania Academic Clinic of Pediatrics, Tbilisi State Medical University, Tbilisi, Georgia

[3]Cologne Center for Genomics, University of Cologne, Cologne, Germany

[4]Department of Pediatrics, University of Bonn, School of Medicine & University Hospital Bonn, Bonn, Germany

[5]Department of Dermatology, Medical Center - University of Freiburg, Faculty of Medicine, University of Freiburg, Freiburg, Germany

[6]Institute of Structural Biology, University of Bonn, School of Medicine, Bonn, Germany

Correspondence
Regina C. Betz, Institute of Human Genetics, University Hospital Bonn, Venusberg-Campus 1, Building 13, D-53127 Bonn, Germany.
Email: regina.betz@uni-bonn.de

Funding information
Deutsche Forschungsgemeinschaft, Grant/Award Number: Germany Excellence Strategy - EXC2151-390873048; German-Israeli Foundation for Scientific Research and Development, Grant/Award Number: I-1443-422.13/2017

KEYWORDS: congenital alopecia, hypotrichosis simplex, intellectual disability, lanosterol synthase, prenatal diagnostics

To the Editor:

The gene *LSS* encodes lanosterol synthase. Previous research has shown that mutations in *LSS* cause congenital cataract (Chen & Liu, 2017; Zhao et al., 2015), as well as autosomal recessive hypotrichosis simplex (HS) or congenital alopecia (Besnard et al., 2019; Chen & Liu, 2017; Li et al., 2019; Romano et al., 2018). These conditions may be accompanied by a neuroectodermal phenotype, such as intellectual disability (ID), epilepsy, microcephaly, genital abnormalities in males, and other dermatological features, such as ichthyosis and erythroderma (Besnard et al., 2019). Wide intra- and interfamilial phenotypic variability is observed, with the former being less pronounced. In particular, one study reported a family in which two affected siblings presented with substantially differing degrees of ID (Besnard et al., 2019). To date, the establishment of a genotype–phenotype correlation for *LSS* mutations has not been possible.

The present report describes four families in which *LSS* mutations led to HS with or without accompanying clinical features. Four of the identified mutations are novel, and one is previously known. Notably, one of the novel mutations is an apparent synonymous mutation, which leads to altered splicing, as demonstrated by cDNA sequencing.

The seven-year-old daughter of first-degree cousins from Iraq (family 1) presented with a lifetime history of sparse hair, which grew to a maximum length of 1 cm (Figure 1a). Her eyelashes and eyebrows were unremarkable, and no abnormalities of the skin or nails were observed. The child also presented with a developmental speech disorder, learning difficulties, and microcephaly. Whole exome sequencing revealed the homozygous substitution c.530G > A (p.Arg177Gln) (rs142081800, gnomAD v.2.1.1 frequency = 5.66e-5) in *LSS* (NM_002340). Both parents were heterozygous carriers of the mutation (Figure 1a). Recent studies reported this mutation occurring in a compound heterozygous state, together with other mutations, in two further hypotrichosis patients,

F. Buket Basmanav and Regina C. Betz have contributed equally to this study.

This is an open access article under the terms of the Creative Commons Attribution-NonCommercial-NoDerivs License, which permits use and distribution in any medium, provided the original work is properly cited, the use is non-commercial and no modifications or adaptations are made.
© 2021 The Authors. *American Journal of Medical Genetics Part A* published by Wiley Periodicals LLC.

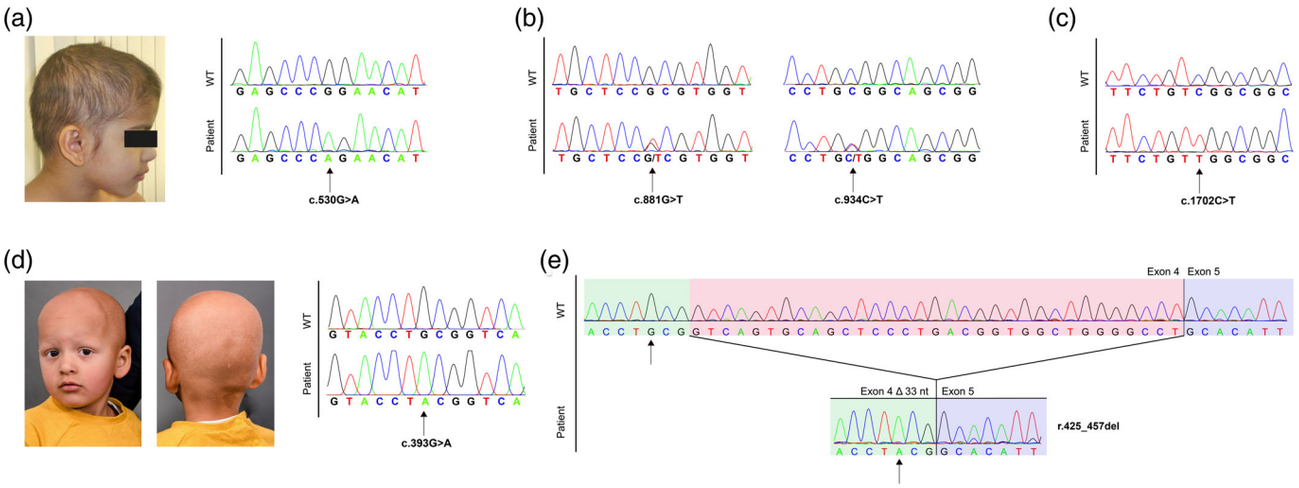

FIGURE 1 Clinical phenotypes and mutation analyses. (a) The 7-year-old girl of Iraqi descent presented with a lifetime history of sparse hair. Mutation analysis by Sanger sequencing revealed that she carries the previously reported missense mutation, c.530G > A (p.Arg177Gln), in homozygous state. (b) Mutation analysis in the two Georgian siblings and their family members revealed that they both carry the previously unreported missense mutations c.934C > T (p.Arg312Trp) and c.881G > T (p.Arg294Leu) in a compound heterozygous state. (c) Mutation analysis in the 9-year old girl from Syria showed that she carries the previously unreported missense mutation c.1702C > T (p.Arg568Trp) in a homozygous state. (d) The 3-year-old boy of Afghani descent presented with total lack of scalp hair, eyebrows as well as body hair. He had very sparse eyelashes. Mutation analyses revealed that he carries the synonymous variant c.393G > A (p.131Leu=) in a homozygous state. (e) Sanger sequencing of cDNA reverse transcribed from RNA that had been isolated from the blood of the Afghani boy, revealed that the synonymous variant c.393G > A (p.131Leu=) leads to activation of a cryptic donor site, which eventually results in skipping of exon 4 and an in frame deletion of 33 nucleotides corresponding to 11 amino acid residues

who presented with and without ID, respectively (Murata et al., 2021; Wada et al., 2020).

Two siblings from Georgia (a boy aged 7 years and a girl aged 14 years, family 2), presented with a complete lack of scalp hair. Although both siblings had shown some degree of scalp hair growth from the age of 5 years, the hair had subsequently fallen out. Both siblings presented with sparse and very light colored eyelashes and eyebrows, and some fine hairs were evident on the back, legs, and hands. The mother described the mental development of the girl as normal. However, she reported that the boy had hearing difficulties, and experienced concentration problems at school, which has not yet been formally evaluated. Whole exome sequencing revealed that both siblings carry the mutations c.934C > T (p.Arg312Trp) (rs764497439, gnomAD v.2.1.1 frequency = 2.82e-5) and c.881G > T (p.Arg294Leu) (rs188459967, gnomAD v.2.1.1 frequency = 8.1e-6) in *LSS* in a compound heterozygous state (Figure 1b). The mutations co-segregate with the disease phenotype in the family. The healthy parents carry each one of the mutations in a heterozygous state.

The nine-year old daughter of consanguineous parents from Syria (family 3) presented at the age of 5 years with a history of very sparse scalp hair from birth. Her younger brother was similarly affected. The parents reported that after episodes of febrile illness, a diffuse loss of scalp hair always occurred, with subsequent spontaneous regrowth. DNA was only available from the girl. Mutation analysis of *LSS* by Sanger sequencing revealed the homozygous missense mutation c.1702C > T (p.Arg568Trp) (rs769430360) (Figure 1c).

The 3-year-old son of first-degree cousins of Afghani descent (family 4) presented with total alopecia. The parents reported that although he had had scant fluffy hair on the scalp at birth, this had fallen out completely by the age of 2 months. The child presented with missing eyebrows and body hair, and very sparse eyelashes (Figure 1d). The skin on his arms was dry, with an appearance that resembled keratosis pilaris. No other cutaneous or neurodevelopmental abnormalities were observed. Sanger sequencing revealed the synonymous variant c.393G > A (p.131Leu=) in *LSS* in a homozygous state (Figure 1d). Both parents were heterozygous for the mutation, which was predicted to be "disease causing" by Mutation Taster. In silico analysis for splice site effects was performed using HSF Pro (Desmet et al., 2009) and SpliceAI (Jaganathan et al., 2019). Both analyses predicted that the mutation caused the activation of a cryptic donor site. This prediction was assessed via cDNA sequencing, which involved the isolation of RNA from the boy's blood cells and reverse transcription. The results confirmed that the mutation leads to the activation of the in silico predicted cryptic donor site 2 bp adjacent to the substitution, which eventually leads to partial skipping of exon 4 and an in frame deletion of 11 amino acid residues: r.425-457del (Figure 1e).

Based on the crystal structure of the human lanosterol synthase (PDB accession code 1W6K) (Thoma et al., 2004), the disease related mutations identified in this study were modeled into the structure and analyzed for their potential impact on the structural integrity of the synthase and its enzymatic function (Figure 2). This analysis showed

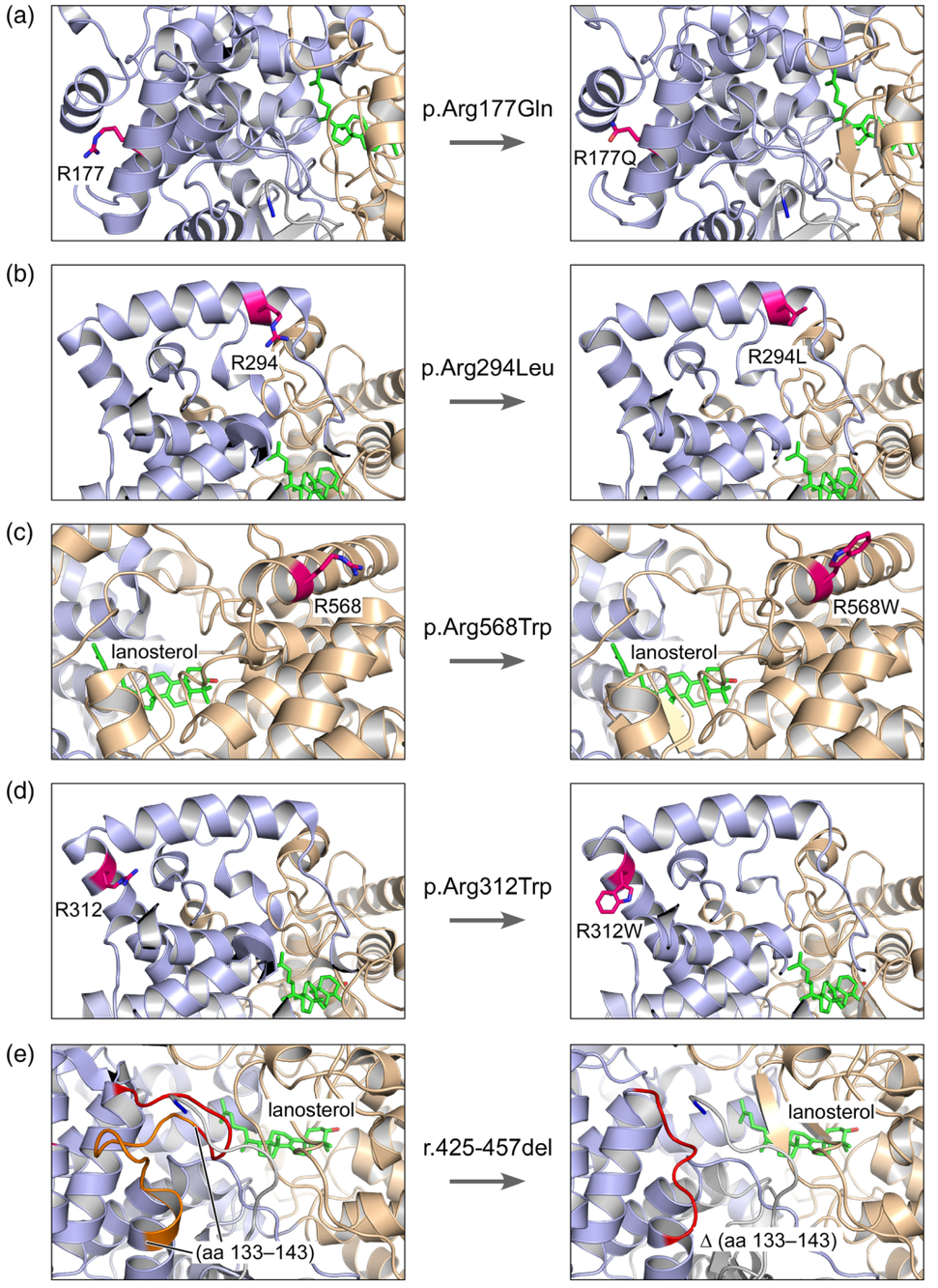

Ex4: c.393G>A, g.6160G>A homozygot, no amino acid changes

```
Patient   101 PLFLLPGLLITCHVARIPLPAGYREEIVRYLR----------HIEDKST   150
              |||||||||||||||||||||||||||||||||          |||||||
Native    101 PLFLLPGLLITCHVARIPLPAGYREEIVRYLRSVQLPDGGWGLHIEDKST   150
```

FIGURE 2 The three point substitutions (a) Arg177Gln in family 1, (b) Arg294Leu in family 2, and (c) Arg568Trp in family 3, are all located on the surface of the protein. (d) The Arg312Trp mutation in family 2 resides within a kink between an amphipathic helix (aa 290–306), that was suggested to be part of a membrane insertion region (Thoma et al., 2004), and the following helix. (e) The deletion mutation Δ(aa 133–143) found in family 4 is located in the first (α/α)-barrel domain of the synthase toward the C-terminal end of a helix (aa 122–135) and an extended linker region (aa 136–150). Modeling of this deletion allowed to connect the two helices (aa 122–132 and aa 150–164) with the remaining residues 144–149 that now adopt a rather straight instead of a meandered conformation. aa: amino acid

that all mutations might have consequences on the three-dimensional structure of the protein, however, none appeared to be deleterious on the protein and its enzymatic activity. Families 1–3 each have a mutation either in homozygous (families 1 and 3) or compound heterozygous state (family 2) leading to the substitution of a surface exposed arginine. These positively charged residues may be involved in interacting with the negatively charged lipid surface and their substitution could therefore, influence the membrane association of the enzyme (Figure 2a–c). Family 2 carries an additional mutation that leads to the substitution of an arginine residue located in the close proximity of a putative membrane insertion region by a tryptophan. This substitution could change the local arrangement of the membrane insertion region and thus influence lanosterol substrate uptake (Figure 2d). Finally, the mutation that leads to the deletion of 11 amino acid residues in family 4 may have an effect on the local arrangement of the helices surrounding the lanosterol binding site and therefore, it may influence, even if not substantially, the catalytic activity of the synthase.

All *LSS* mutations reported to date have been missense, nonsense, or splice site mutations, and no synonymous *LSS* mutation has yet been reported to cause HS with or without neurodevelopmental abnormalities. Based on our discovery of the pathogenic synonymous variant, which leads to aberrant splicing, we propose that the possible molecular consequences of all identified synonymous *LSS* mutations in patients should be carefully investigated before their pathogenicity is ruled out.

With respect to genotype–phenotype correlations, it remains unclear which mutations in *LSS* lead to an alopecia phenotype only, and which lead to accompanying severe neurodevelopmental and dermatological phenotypes. At writing, we hypothesize that the presence and extent of such additional clinical features may be related to the degree of normal protein function. Further functional studies are warranted to understand the mechanisms underlying the phenotypic variability that arises from *LSS* mutations.

At writing, the general (but not fixed) consensus is that prenatal diagnostics (PD) should not be offered for alopecia alone. However, given the reported interfamilial phenotypic variability (Besnard et al., 2019), the siblings of children with an alopecia only phenotype may display cognitive disability and/or a severe skin phenotype. Therefore, we must be prepared to offer PD for future pregnancies in cases where the parents are both known *LSS* mutation carriers or who already have an affected child.

The identification of further *LSS* mutation carriers will facilitate our understanding of this complex and unpredictable protein. This in turn will improve predictions concerning the phenotypic outcomes of individual *LSS* mutations.

ACKNOWLEDGMENTS

The authors thank all family members for their participation. This study was supported by the grant I-1443-422.13/2017 (to Regina C. Betz) from the German-Israeli Foundation for Scientific Research and Development (GIF), and a grant (to Regina C. Betz and Matthias Geyer) from the Deutsche Forschungsgemeinschaft (DFG, German Research Foundation), under the auspices of the Germany Excellence Strategy—EXC2151-390873048.

CONFLICT OF INTEREST

The authors declare no conflict of interest.

AUTHOR CONTRIBUTIONS

Nicole Cesarato, Maria Wehner, Daisy Axt, and Holger Thiele contributed to the sequencing experiments and mutation analysis; Mariam Ghughunishvili, Cristina Has, and Michael J. Lentze collected clinical data and blood samples, Axel Schmidt performed bioinformatic analysis, Matthias Geyer performed structural protein modeling and contributed to the writing of the article, F. Buket Basmanav performed data analysis, supervised the study and wrote the manuscript. Regina C. Betz collected clinical data, supervised the study and wrote the manuscript.

DATA AVAILABILITY STATEMENT

Data are presented in the manuscript. Additional information such as experimental conditions are available upon request.

ORCID

Fitnat Buket Basmanav https://orcid.org/0000-0001-6411-4275
Regina C. Betz https://orcid.org/0000-0001-5024-3623

REFERENCES

Besnard, T., Sloboda, N., Goldenberg, A., Kury, S., Cogne, B., Breheret, F., Trochu, E., Conrad, S., Vincent, M., Deb, W., Balguerie, X., Barbarot, S., Baujat, G., Ben-Omran, T., Bursztejn, A-C., Carmignac, V., Datta, A. N., Delignières, A., Faivre, L., … Isidor, B. (2019). Biallelic pathogenic variants in the lanosterol synthase gene LSS involved in the cholesterol biosynthesis cause alopecia with intellectual disability, a rare recessive neuroectodermal syndrome. *Genetics in Medicine*, *21*(9), 2025–2035. https://doi.org/10.1038/s41436-019-0445-x

Chen, X., & Liu, L. (2017). Congenital cataract with LSS gene mutations: A new case report. *Journal of Pediatric Endocrinology & Metabolism*, *30* (11), 1231–1235. https://doi.org/10.1515/jpem-2017-0101

Desmet, F. O., Hamroun, D., Lalande, M., Collod-Beroud, G., Claustres, M., & Beroud, C. (2009). Human splicing finder: An online bioinformatics tool to predict splicing signals. *Nucleic Acids Research*, *37*(9), e67. https://doi.org/10.1093/nar/gkp215

Jaganathan, K., Kyriazopoulou Panagiotopoulou, S., McRae, J. F., Darbandi, S. F., Knowles, D., Li, Y. I., Kosmicki, J. A., Arbelaez, J., Cui, W., Schwartz, G. B., Chow, E. D., Kanterakis, E., Gao, H., Kia, A., Batzoglou, S., Sanders, S. J., & Farh, K. K. (2019). Predicting splicing from primary sequence with deep learning. *Cell*, *176*(3), 535–548 e524. https://doi.org/10.1016/j.cell.2018.12.015

Li, F., Liao, C., Li, R., Zhang, Y., Jing, X., Li, Y., & Deng, W. (2019). A novel and a known mutation in LSS gene associated with hypotrichosis 14 in a Chinese family. *The Journal of Dermatology*, *46*(11), e393–e395. https://doi.org/10.1111/1346-8138.15010

Murata, M., Hayashi, R., Kawakami, Y., Morizane, S., & Shimomura, Y. (2021). Two cases of severe congenital hypotrichosis caused by compound heterozygous mutations in the LSS gene. *The Journal of Dermatology*, *48*(3), 392–396. https://doi.org/10.1111/1346-8138.15679

Romano, M. T., Tafazzoli, A., Mattern, M., Sivalingam, S., Wolf, S., Rupp, A., Thiele, H., Altmüller, J., Nürnberg, P., Ellwanger, J., Gambon, R., Baumer, A., Kohlschmidt, N., Metze, D., Holdenrieder, S., Paus, R., Lütjohann, D., Frank, J., Geyer, M., … Betz, R. C. (2018). Bi-allelic mutations in LSS, encoding lanosterol synthase, cause autosomal-recessive

hypotrichosis simplex. *American Journal of Human Genetics*, *103*(5), 777–785. https://doi.org/10.1016/j.ajhg.2018.09.011

Thoma, R., Schulz-Gasch, T., D'Arcy, B., Benz, J., Aebi, J., Dehmlow, H., Hennig, M., Stihle, M., & Ruf, A. (2004). Insight into steroid scaffold formation from the structure of human oxidosqualene cyclase. *Nature*, *432*(7013), 118–122. https://doi.org/10.1038/nature02993

Wada, Y., Kikuchi, A., Kaga, A., Shimizu, N., Ito, J., Onuma, R., Fujishima, F., Totsune, E., Sato, R., Niihori, T., Shirota, M., Funayama, R., Sato, K., Nakazawa, T., Nakayama, K., Aoki, Y., Aiba, S., Nakagawa, K., & Kure, S. (2020). Metabolic and pathologic profiles of human LSS deficiency recapitulated in mice. *PLoS Genetics*, *16*(2), e1008628. https://doi.org/10.1371/journal.pgen.1008628

Zhao, L., Chen, X. J., Zhu, J., Xi, Y. B., Yang, X., Hu, L. D., Ouyang, H., Patel, S. H., Jin, X., Lin, D., Wu, F., Flagg, K., Cai, H., Li, G., Cao, G., Lin, Y., Chen, D., Wen, C., Chung, C., … Zhang, K. (2015). Lanosterol reverses protein aggregation in cataracts. *Nature*, *523*(7562), 607–611. https://doi.org/10.1038/nature14650

How to cite this article: Cesarato, N., Wehner, M., Ghughunishvili, M., Schmidt, A., Axt, D., Thiele, H., Lentze, M. J., Has, C., Geyer, M., Basmanav, F. B., & Betz, R. C. (2021). Four hypotrichosis families with mutations in the gene *LSS* presenting with and without neurodevelopmental phenotypes. *American Journal of Medical Genetics Part A*, *185*A:3900–3904. https://doi.org/10.1002/ajmg.a.62438

4. Discussion with references

4.1 The importance of research on hair disorders

Genetic studies of monogenic hair disorders are a method of identifying genes that are essential for the HF development and function. These genes encode for proteins that are of such critical importance that their dysregulation has a severe impact on hair morphogenesis, growth, and/or cycle, ultimately resulting in HF dysfunction.

In general, the discovery of new variants and genes with an association to hair disorders has multiple outcomes. First, it provides new molecular diagnostic tools to facilitate the correct diagnosis of hair diseases. Second, it improves understanding of the underlying biology of the HF as a complex mini-organ. Third, it leads to the identification of the molecular pathways that are involved in hair loss/hair growth. Modulation of the activity of the affected pathways on the physiological level represents a possible pharmaceutical strategy to cure hair disorders. In fact, despite the high prevalence of hair disorders in the population, only few therapies are available for multifactorial hair disorders and none for monogenic forms (Harrison und Sinclair, 2003; Nestor et al., 2021).

4.1.1 *WNT10A* variants in short anagen hair syndrome and male pattern hair loss

Our study on SAH is the first to describe the genetic background of SAH, and is currently the largest SAH cohort to have been reported in the literature (Cesarato et al., in press). We analysed 48 individuals presenting with SAH or complaints suggestive of SAH, and found an enrichment of low-frequency *WNT10A* pathogenic variants in the SAH cohort compared to the general population.

Prior to our study, the crucial role of *WNT10A* in all ectodermal appendages - in particular teeth and the HF - had already been demonstrated via extensive research in both *in vitro* and *in vivo* models (Hawkshaw et al., 2020; Xu et al., 2017). Research suggests that individuals who are heterozygous carriers of *WNT10A* variants may show a sex-biased phenotype, predominantly tooth disorders in males, and hair or nail abnormalities in females (Bohring et al., 2009; Doolan et al., 2021). However, no *WNT10A*-specific hair phenotype had ever been described. Our research is thus the first to determine a *WNT10A*-specific hair phenotype, namely SAH. We propose that SAH can occur as either a previously under-recognised feature of *WNT10A*-related ED in biallelic carriers, or as an isolated clinical feature in heterozygous carriers.

A role of *WNT10A* in MPHL aetiopathogenesis had been previously described (Heilmann et al., 2013). In our SAH study, we also found a significant association between two SAH-associated *WNT10A* variants and MPHL. The discovery of a genetic overlap between two hair disorders that differ in terms of inheritance pattern, lifetime occurrence, and sex prevalence was intriguing. A shared trait of both disorders is the reduced length of the anagen phase of the HF. Previous authors have hypothesised that WNT10A plays a role in anagen induction and maintenance (Hawkshaw et al., 2020; Hochfeld et al., 2021; Xu et al., 2017), and our study supports this. Our study also suggests that WNT10A-mediated wnt signalling might be a drug target for anagen elongation.

4.1.2 Genetic spectrum of uncombable hair syndrome

In the UHS study, we analysed the genetic spectrum of UHS in a cohort of 107 individuals from 20 different countries (Basmanav et al., 2022).

The results of this study help prioritize genes for sequencing in individuals presenting with UHS who seek dermatological and/or genetic consultation. We showed that in affected individuals presenting with UHS, sequencing of *PADI3* should be prioritised, in particular exons 3 and 8, where the most common causative variants - p.(Ala294Val) and p.(Leu112His) - are located. If pathogenic variants cannot be identified, on the basis of our results, we recommend that all exons of *PADI3* should be sequenced, followed by sequencing of *TGM3* and *TCHH*.

For 25 % of the UHS cohort, the genetic cause remained unexplained, despite the availability of whole exome sequencing (WES) data for most individuals. Two of these individuals had heterozygous *TCHH* loss of function variants. These findings pointed to the possibility that in these individuals, a second pathogenic variant might be present in *TCHH*, such as a copy number variation (CNV) that was undetectable via WES. However, given the low number of unexplained cases with heterozygous variants in *PADI3*, *TGM3*, and *TCHH*, CNV analysis would only clarify a small number of unsolved cases. Due to the availability of the WES data, we can also postulate that the presence of a fourth gene, whose variants cause the majority of the unexplained UHS cases, is unlikely. In contrast, the presence of multiple causative genes, each explaining a small fraction of UHS cases, as with *TCHH* and *TGM3*, is likely. Therefore, the analysis of a larger UHS cohort might facilitate the discovery of additional causal genes for UHS.

4.1.3 Genotype-phenotype correlation of *LSS* variants

In the *LSS* paper, we described the genetic investigation of four individuals presenting with hypotrichosis with or without intellectual disability (Cesarato et al., 2021). Pathogenic variants in *LSS* are associated with a spectrum of anomalies that have differing degrees of severity, ranging from HS to the severe palmoplantar keratoderma-congenital alopecia syndrome. Although the genotype-phenotype correlation of *LSS* variants remains unclear, a new hypothesis on a possible genotype-phenotype correlation has been formulated. In particular, two recent papers analysed all published *LSS* variants, comprising ours, and showed that splicing, stop, and frameshift variants are enriched in individuals presenting with more severe phenotypes. Therefore, the authors proposed that disease severity is related to the residual activity of LSS (Elbendary et al., 2023; Guo und Zhang, 2023). These studies demonstrate once more the importance of cholesterol homeostasis in HF morphogenesis and growth (Palmer et al., 2020).

4.2 Perspectives for the genetic elucidation of hair disorders

Despite current advances in the study of monogenic hair disorders, many cases in our SAH, UHS, and HS cohorts remain genetically unexplained.

Currently, WES is the most commonly applied technique in the genetic elucidation of monogenic hair disorders. However, WES is restricted to the analysis of SNVs and small deletions and duplications in coding regions of the genome, and thus only around 1.5 % of the genome is covered when this technique is applied. Although more expensive, whole genome sequencing allows the analysis of non-coding regions and thus enables the identification of: (i) deep intronic variants and CNVs in known hair related genes; and (ii) new genetic loci in non-coding regions of importance for hair growth. A proof of principle of the latter is the pathogenicity of variants in *U2HR*, an inhibitory regulatory region upstream of the hairless (*HR*) gene. *U2HR* is causative for the monogenic hair disorder Marie Unna hypotrichosis (Wen et al., 2009). The use of long read sequencing might be particularly useful in terms of resolving the sequence of genes containing repeated regions, for example *TCHH* (Lee et al., 1993).

Moreover, RNA sequencing (RNAseq) and single cell RNA sequencing might be future methods of choice with respect to: (i) gaining a deeper understanding of signalling pathways; and (ii) mapping which particular cell types are affected by specific hair

disorders. Analysis of the HF transcriptome of genetically unexplained cases could highlight which dysregulated pathways are specific for certain hair conditions, and therefore facilitate the identification of novel causal genetic loci for these disorders. The identification of dysregulated pathways that are common to multiple hair conditions could allow the design of new pharmaceutical entities that are effective in diverse hair disorders. In summary, the application of novel technologies in the genetic hair disorder field could help not only in terms of diagnostics, but also in terms of hair biology research and drug discovery. This in turn would improve the quality of life of affected individuals.

4.3 References

Basmanav FB, Cesarato N, Kumar S, Borisov O, Kokordelis P, Ralser DJ, Wehner M, Axt D, Xiong X, Thiele H, Dolgin V, Gossmann Y, Fricker N, Dewenter MK, Weller K, Suri M, Reichenbach H, Oji V, Addor MC, Ramirez K, Stewart H, Garcia Bartels N, Weibel L, Wagner N, George S, Kilic A, Tantcheva-Poor I, Stewart A, Dikow N, Blaumeiser B, Medvecz M, Blume-Peytavi U, Farrant P, Grimalt R, Bertok S, Bradley L, Eskin-Schwartz M, Birk OS, Bygum A, Simon M, Krawitz P, Fischer C, Hamm H, Fritz G, Betz RC. Assessment of the Genetic Spectrum of Uncombable Hair Syndrome in a Cohort of 107 Individuals. JAMA Dermatol. 2022; 158: 1245-1253

Bohring A, Stamm T, Spaich C, Haase C, Spree K, Hehr U, Hoffmann M, Ledig S, Sel S, Wieacker P, Ropke A. WNT10A mutations are a frequent cause of a broad spectrum of ectodermal dysplasias with sex-biased manifestation pattern in heterozygotes. Am J Hum Genet. 2009; 85: 97-105

Cesarato N, Schwieger-Briel A, Gossmann Y, Henne SK, Hillmann K, Frommherz LH, Wehner M, Xiong X, Thiele H, Oji V, Milani D, Tantcheva-Poor I, Giehl K, Folster-Holst R, Teichler A, Braeckmans D, Hoeger PH, Jones G, Frank J, Weibel L, Blume-Peytavi U, Hamm H, Nothen MM, Geyer M, Heilmann-Heimbach S, Basmanav FB, Betz RC. Short anagen hair syndrome: Association with mono- and biallelic variants in WNT10A and a genetic overlap with male pattern hair loss. Br J Dermatol. Epub ahead of print

Cesarato N, Wehner M, Ghughunishvili M, Schmidt A, Axt D, Thiele H, Lentze MJ, Has C, Geyer M, Basmanav FB, Betz RC. Four hypotrichosis families with mutations in the gene LSS presenting with and without neurodevelopmental phenotypes. Am J Med Genet A. 2021; 185: 3900-3904

Doolan BJ, Onoufriadis A, Kantaputra P, McGrath JA. WNT10A, dermatology and dentistry. Br J Dermatol. 2021; 185: 1105-1111

Elbendary HM, Marafi D, Saad AK, Elhossini R, Duan R, Rafat K, Jhangiani SN, Gibbs RA, Pehlivan D, Calame DG, Posey JE, Lupski JR, Zaki MS. Novel LSS variants in alopecia and intellectual disability syndrome: New case report and clinical spectrum of LSS-related rare disease traits. Clin Genet. 2023; 104: 344-349

Guo D, Zhang Q. A case of LSS-associated congenital nuclear cataract with hypotrichosis and literature review. Am J Med Genet A. 2023; 191: 2398-2401

Harrison S, Sinclair R. Optimal management of hair loss (alopecia) in children. Am J Clin Dermatol. 2003; 4: 757-770

Hawkshaw NJ, Hardman JA, Alam M, Jimenez F, Paus R. Deciphering the molecular morphology of the human hair cycle: Wnt signalling during the telogen-anagen transformation. Br J Dermatol. 2020; 182: 1184–1193

Heilmann S, Kiefer AK, Fricker N, Drichel D, Hillmer AM, Herold C, Tung JY, Eriksson N, Redler S, Betz RC, Li R, Kárason A, Nyholt DR, Song K, Vermeulen SH, Kanoni S, Dedoussis G, Martin NG, Kiemeney LA, Mooser V, Stefansson K, Richards JB, Becker T, Brockschmidt FF, Hinds DA, Nöthen MM. Androgenetic alopecia: identification of four genetic risk loci and evidence for the contribution of WNT signaling to its etiology. J Invest Dermatol. 2013; 133: 1489–1496

Hochfeld LM, Bertolini M, Broadley D, Botchkareva NV, Betz RC, Schoch S, Nothen MM, Heilmann-Heimbach S. Evidence for a functional interaction of WNT10A and EBF1 in male-pattern baldness. PLoS One. 2021; 16: e0256846

Lee SC, Kim IG, Marekov LN, O'Keefe EJ, Parry DA, Steinert PM. The structure of human trichohyalin. Potential multiple roles as a functional EF-hand-like calcium-binding protein, a cornified cell envelope precursor, and an intermediate filament-associated (cross-linking) protein. J Biol Chem. 1993; 268: 12164-12176

Nestor MS, Ablon G, Gade A, Han H, Fischer DL. Treatment options for androgenetic alopecia: Efficacy, side effects, compliance, financial considerations, and ethics. J Cosmet Dermatol. 2021; 20: 3759-3781

Palmer MA, Blakeborough L, Harries M, Haslam IS. Cholesterol homeostasis: Links to hair follicle biology and hair disorders. Exp Dermatol. 2020; 29: 299-311

Wen Y, Liu Y, Xu Y, Zhao Y, Hua R, Wang K, Sun M, Li Y, Yang S, Zhang X-J, Kruse R, Cichon S, Betz RC, Nöthen MM, van Steensel MAM, van Geel M, Steijlen PM, Hohl D, Huber M, Dunnill GS, Kennedy C, Messenger A, Munro CS, Terrinoni A, Hovnanian A, Bodemer C, Prost Yd, Paller AS, Irvine AD, Sinclair R, Green J, Shang D, Liu Q, Luo Y, Jiang L, Chen H-D, Lo WH-Y, McLean WHI, He C-D, Zhang X. Loss-of-function mutations of an inhibitory upstream ORF in the human hairless transcript cause Marie Unna hereditary hypotrichosis. Nat genet. 2009; 41: 228–233

Xu M, Horrell J, Snitow M, Cui J, Gochnauer H, Syrett CM, Kallish S, Seykora JT, Liu F, Gaillard D, Katz JP, Kaestner KH, Levin B, Mansfield C, Douglas JE, Cowart BJ, Tordoff M, Liu F, Zhu X, Barlow LA, Rubin AI, McGrath JA, Morrisey EE, Chu EY, Millar SE. WNT10A mutation causes ectodermal dysplasia by impairing progenitor cell proliferation and KLF4-mediated differentiation. Nat Commun. 2017; 8: 15397

5. Acknowledgement

This thesis was not the effort of a single person, but rather the outcome of extensive work involving the collaboration and support of many people, all of whom deserve special mention.

First, I would like to thank my supervisor, Prof. Regina Betz, for her knowledge, dedication, patience, and support during my five years in her lab. In particular, I am grateful for her trust, for always valuing my opinion, and for allowing me to pursue my own areas of interest in the genetic and hair research fields.

I also extend my sincere thanks to all of my colleagues, for all of the lunchtimes spent together, the help, the gossip, the exchange of opinions, the scientific and personal conversations, and, of course, for all the fun times we shared. In particular, I thank Dr. Buket Basmanav, who took the time and effort to accompany me in the field of multifactorial disorders, and who opened my eyes to multiple new perspectives.

I thank the whole Institute of Human Genetics in Bonn, in particular its director, Prof. Markus Nöthen, and the members of the commission. There, discussions, journal clubs, and progress reports allowed me to grow as a scientist.

I thank all of the people that I met in Bonn, all of my friends in Italy and across Europe, my boyfriend, and my family. I would be lost without them. In particular, I thank the people who were there when things were so bad I could not sleep, and when things were so good they deserved celebration.

Finally, I extend my thanks to you, the reader, for taking the time to enter with me into the beautiful world of the hair follicle, with all its perfection and complexity.